LaViDa: A Large Diffusion Language Model for Multimodal Understanding

Shufan Li[1*], **Konstantinos Kallidromitis**[2*], **Hritik Bansal**[1*], **Akash Gokul**[4*], **Yusuke Kato**[2]
Kazuki Kozuka[2], **Jason Kuen**[3], **Zhe Lin**[3], **Kai-Wei Chang**[1], **Aditya Grover**[1]
[1]UCLA [2]Panasonic AI Research [3]Adobe Research [4]Salesforce Research
* Equal Contribution

Abstract

Modern Vision-Language Models (VLMs) can solve a wide range of tasks requiring visual reasoning. In real-world scenarios, desirable properties for VLMs include fast inference and controllable generation (e.g., constraining outputs to adhere to a desired format). However, existing autoregressive (AR) VLMs like LLaVA struggle in these aspects. Discrete diffusion models (DMs) offer a promising alternative, enabling parallel decoding for faster inference and bidirectional context for controllable generation through text-infilling. While effective in language-only settings, DMs' potential for multimodal tasks is underexplored. We introduce LaViDa, a family of VLMs built on DMs. We build LaViDa by equipping DMs with a vision encoder and jointly fine-tune the combined parts for multimodal instruction following. To address challenges encountered, LaViDa incorporates novel techniques such as complementary masking for effective training, prefix KV cache for efficient inference, and timestep shifting for high-quality sampling. Experiments show that LaViDa achieves competitive or superior performance to AR VLMs on multi-modal benchmarks such as MMMU, while offering unique advantages of DMs, including flexible speed-quality tradeoff, controllability, and bidirectional reasoning. On COCO captioning, LaViDa surpasses Open-LLaVa-Next-Llama3-8B by +4.1 CIDEr with 1.92× speedup. On bidirectional tasks, it achieves +59% improvement on Constrained Poem Completion. These results demonstrate LaViDa as a strong alternative to AR VLMs. Code and models is available at https://github.com/jacklishufan/LaViDa

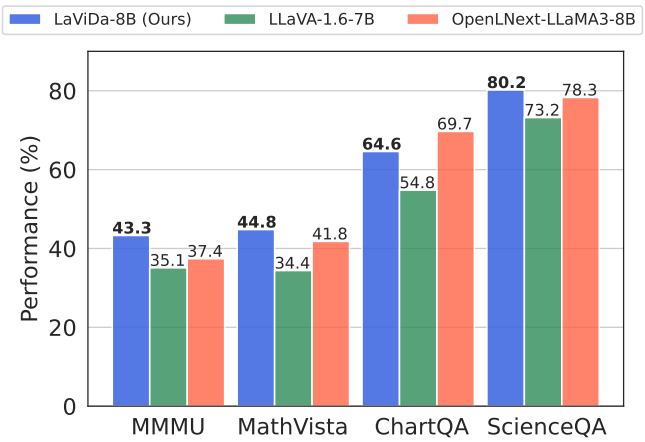

Figure 1: **We propose LaViDa,** the first family of diffusion-based discrete VLM models. LaViDa models achieve competitive performance against AR baselines (LLaVa-1.6, Open-LLaVa-Next) across multiple visual understanding tasks including MMMU (world knowledge), MathVista (reasoning), ChartQA (OCR), and ScienceQA (science).

39th Conference on Neural Information Processing Systems (NeurIPS 2025).

1 Introduction

Vision-Language Models (VLMs) have shown remarkable utility across diverse domains, from end-user applications like virtual assistants [37], to research tasks such as scientific image captioning and document understanding [46, 16, 5, 1, 48]. In industrial settings, VLMs support automated product tagging, content moderation, and quality control in manufacturing [69, 2]. Their ability to jointly process visual and textual information makes them indispensable for practical applications and cutting-edge research. Currently, nearly all popular VLMs—such as Qwen-VL [5, 75], Intern-VL [17, 85], and GPT-4 [58] are built on top of large language models (LLMs) that generate text in an autoregressive (AR) manner; that is, they produce tokens one by one in a left-to-right sequence.

While these models have demonstrated strong performance on many tasks, they suffer from several key limitations. First, their sequential generation process is inherently hard to parallelize, resulting in slow inference speed [8]. More critically, their left-to-right generation makes it difficult to handle tasks that benefit from bidirectional context or structural constraints—such as text infilling [22]. For example, generating a poem where each line starts with a specific syllable, or extracting structured information from an image in a predefined JSON format, often requires the model to fill in or coordinate content across the sequence. Autoregressive models still struggle to consistently satisfy such constraints, even with carefully crafted prompts and examples.

Recently, discrete diffusion models (DMs) have emerged as a promising alternative to AR LLMs. Most notably, LLaDA [57] and Dream [79] achieved comparable results to AR LLMs across diverse language tasks. Unlike AR LLMs, DMs treat text generation as a diffusion process over discrete tokens. A forward process gradually corrupts a sequence of discrete text tokens into a sequence of mask tokens. At inference, we start with a sequence of mask tokens and gradually transform them into a sequence of meaningful text tokens through a learned reverse process.

Compared to AR LLMs, diffusion models offer several theoretical advantages that directly address the limitations of autoregressive generation. While AR LLMs have a fixed throughput—generating one token at a time—DMs allow flexible control over the speed-quality trade-off by adjusting the number of diffusion steps [79, 64, 49, 57]. Moreover, their ability to model bidirectional context makes them well-suited for tasks like text infilling, enabling more effective constrained generation and structured output formatting—capabilities especially valuable in vision-language settings where outputs may need to follow specific schemas.

In this work, we propose LaViDa (**L**arge **Vi**sion-Language **D**iffusion Model with M**a**sking), the first family of VLMs based on diffusion. LaViDa enables pretrained DMs to perceive visual inputs by integrating vision features into the diffusion backbone via a vision encoder—analogous to how LLaVA [46, 44] augments large language models (LLMs) with visual inputs. Specifically, we adopt a two-stage training pipeline with a diffusion objective: pretraining followed by supervised fine-tuning.

Adapting DMs for vision-language tasks presents several practical challenges. First, standard DM training is data-inefficient: the model learns only from the subset of corrupted tokens at each timestep. For example, in a question-answering task where the target answer is ‘‘`The answer is dog`’’, the corruption process may mask ‘‘`The [mask] is dog`’’, leaving the key token ‘‘`dog`’’ unmasked and thus excluded from the loss. This is especially problematic for multimodal tasks, where answer tokens often carry crucial semantic content grounded in the image [61]. To address this, we introduce a complementary masking scheme that ensures every token in the output sequence contributes to learning, improving data efficiency.

Second, inference algorithms used by existing DMs are slow in practice due to the lack of KV cache support—an inherent limitation of bidirectional context modeling [3]. This leads to repeated recomputation over the full prompt at every decoding step. While tolerable for short-text settings, it becomes a significant bottleneck in vision-language tasks, where multimodal prompts may include hundreds of visual tokens. To address this, we propose Prefix-DLM decoding, a simple yet effective technique that enables caching of multimodal prompts (i.e., image and question tokens), significantly accelerating inference.

Lastly, DMs offer a unique advantage over autoregressive models: the ability to trade off speed and quality by varying the number of diffusion steps. However, the widely used linear masking schedule—which unmasks a fixed number of tokens per step—performs poorly at low step counts. Motivated by text-to-image diffusion models like SD3 [21], we adopt a timestep shifting strategy that

adaptively adjusts how many tokens are unmasked per step. This leads to better sample quality under aggressive step reduction, allowing faster generation without large degradation in quality.

We conducted extensive evaluations of LaViDa across a wide range of vision-language tasks. Results show that LaViDa achieves competitive performance on most benchmarks, including MMMU [80], MathVista [51], ChartQA [53] and ScienceQA [52], when compared with AR VLMs like LLaVa-1.6-7B [45, 43] and Open-LLaVa-Next-Llama3-8B [15]. We highlight these results in Figure 1. On constrained generation tasks, LaViDa greatly outperforms AR baselines (+59% on Poem Completion). It also supports flexible speed-quality tradeoff, achieving higher quality on COCO image captioning (+ 4.1 CIDEr) and a 1.92× speedup [42]. In summary, our contributions are:

- We introduce LaViDa, the first family of VLMs based on diffusion models. Our models achieve competitive performance across a wide range of tasks compared to AR VLMs, while offering the unique benefits of DMs.
- We introduce several novel training and inference techniques for DMs, including complementary masking, Prefix-DLM, and timestep shifting that improve the training efficiency, inference speed, and sample quality of LaViDa.
- We conduct a systematic study of various design choices for adapting DMs to vision-language tasks (e.g. image resolution), offering insights for future work in this direction.

2 Background and Related Works

2.1 Vision-Language Models

Vision-Language Models (VLM) extend the capability of Large Language Models to visual understanding tasks [36, 46, 75, 5, 9, 85, 58]. The common recipe to build a VLM is to start with a strong large language model and combine it with a vision encoder [46, 75]. These VLMs typically undergo multiple stages of training, which can be generally categorized into pretraining and finetuning stages. The pretraining data usually consists of text-image pairs for vision-language alignment, while the finetuning data consists of a wide range of instruction-following tasks. There are several dedicated lines of work focusing on different components of this overarching framework, such as the design of vision encoders [26, 77] and training techniques [41, 72]. To this date, most vision-language models such as LLaVa [46, 36] and Qwen-VL [5, 75] series employ an autoregressive training objective.

2.2 Diffusion Language Models

Diffusion models first emerged as a powerful alternative to GANs for generating continuous data such as images [62, 59, 21]. Early explorations in diffusion language models directly built continuous diffusion models for latent text embeddings [39, 50], with limited success. More recently, discrete diffusion models [4, 64, 49] have proven to be better candidates for language modeling, achieving performance comparable to AR models while offering unique advantages, such as speed-quality tradeoffs and controllability. Most notably, LLaDa-8B and Dream-8B [57, 79] demonstrated that DLMs can achieve competitive performance against AR LLMs at scale.

Formally, given a text sequence of L tokens $X_0 = [X_0^1, X_0^2 ... X_0^L]$, the forward process $q(X_t|X_s)$ gradually converts it to a sequence full of mask tokens "[M]", denoted by $X_1 = [X_1^1, X_1^2 ... X_1^L]$, through the continuous time-interval $[0, 1]$, with $1 \geq t \geq s \geq 0$. A neural network p_θ is used to model the reverse process $p(X_s|X_t)$. The diffusion language modeling objective can be defined as:

$$\mathcal{L}_{\text{DLM}} = -\mathbb{E}_{t,X_0,X_t}\left[\frac{1}{t}\log p_\theta(X_0|X_t)\right] \tag{1}$$

where $\log p_\theta(X_0|X_t)$ is assumed to be factorized into $\prod_{i=1}^{L} p_\theta(X_0^i|X_t)$. At each training step, we sample t uniformly from the interval $[0, 1]$ and sample X_0 from some data distribution $\mathcal{D}$. X_t is then sampled from the forward process $q(X_t|X_0)$. The loss is only computed over the masked tokens in X_t, since $p_\theta(X_0^i|X_t)$ has a closed form representation that does not depend on θ when $X_t^i \neq [M]$. We offer additional background on the details of these formulations in Appendix A.1. We also incorporate addition backgrounds on other relevant literature, such as masked generative models [10, 11] and multimodal diffusion models [68, 38], in Appendix C.

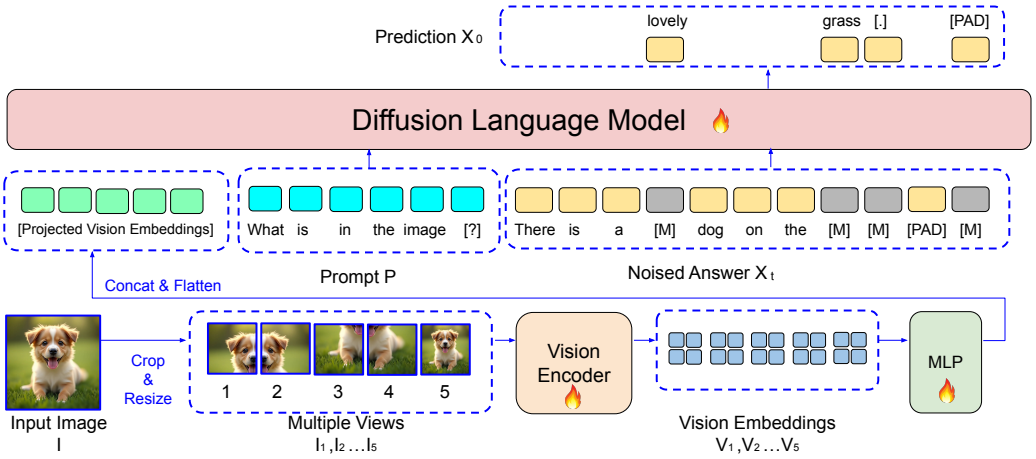

Figure 2: **Overall design of LaViDa.** LaViDa's architecture consists of a vision encoder, a diffusion language model, and an MLP vision projector. The bottom half of the figure illustrates the image encoding process, while the top half depicts the diffusion language modeling process. These two pipelines are described in detail in Sec. 3.1.

3 Method

3.1 Model Architecture

LaViDa's model architecture follows a similar design to common AR VLMs like LLaVa [36]. It consists of a vision encoder and a diffusion language model. These two parts are connected by a MLP projection network. The overall design is illustrated in Figure 2.

Vision Encoder. Given an input image I and text prompt P, we first resize the image to 768^2 and divide it into four non-overlapping views of 384^2, denoted $I_{1:4}$. We also resize the original image to 384^2 to obtain a fifth view, I_5, following the design of prior works [36, 45]. These five views are independently encoded by the vision encoder (SigLIP-400M [82]), each producing 27^2 embeddings, denoted $V_{1:5}$. In total, this yields 3645 embeddings per image. To reduce sequence length for efficient training, we apply 2×2 average pooling on each view, reducing embeddings to 14^2 per view, or 980 total. The embeddings of five views are then flattened and concatenated into a 1D sequence before being processed by the projection network to obtain the final visual context of the diffusion language model. This process mirrors the vision encoding process in AR LLMs [26] and is illustrated in the bottom part of Figure 2.

Diffusion Language Model. The diffusion language model is a multi-layer Transformer [71] whose architecture resembles that of LLMs. The only major difference is that its attention mask is non-causal, and it uses the diffusion language modeling objective described in Section 2.2 instead of the next-token prediction used in AR models. The input to the diffusion language model consists of the projected vision embeddings, the prompt P, and partially masked response X_t. The outputs of the last transformer block are passed through a final linear layer to obtain token-wise logits $p_\theta(X_0^i|I, P, X_t)$ for the unmasked response X_0. In our experiments, we explored LLaDA-8B (default) and Dream-7B as our diffusion language model. This process is illustrated in the upper half of Figure 2.

3.2 Training Algorithms

Our training objective is based on the diffusion language modeling objective described in Section 2.2. Each training sample consists of an image I, text prompt P and clean text answer X_0 from the training data. For multi-round conversation, we sample one round as the "answer" and treat the history as "prompt". We first sample a timestep $t \in [0, 1]$ and a partially masked answer X_t using the forward process described in Section 2.2. LaViDa then implements the conditioned reverse process $p_\theta(X_0|I, P, X_t)$. The canonical diffusion vision-language modeling objective is formulated as:

$$\mathcal{L}_{\text{D-VLM}} = -\mathbb{E}_{t,I,P,X_0,X_t}\left[\frac{1}{t}\log p_\theta(X_0|I, P, X_t)\right] \tag{2}$$

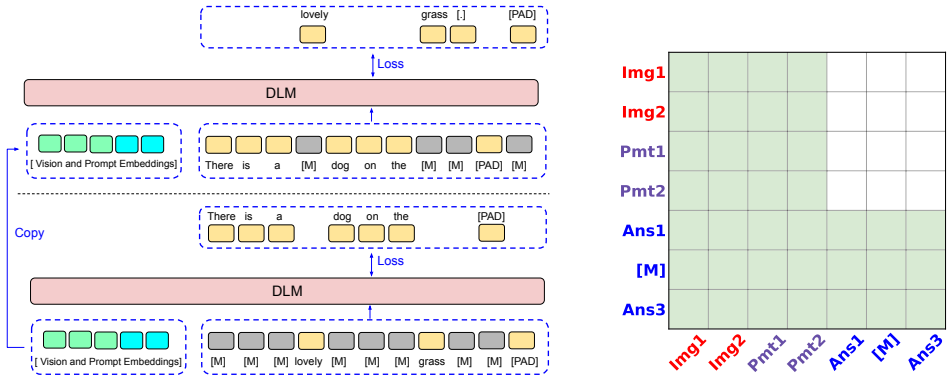

(a) Complementary Masking

(b) Attention Mask of Prefix-DLM

Figure 3: **Technical Details of LaViDa.** (a) We propose Complementary Masking to ensure loss is calculated over all tokens in the data for training efficiency. (b) We propose Prefix-DLM attention mask that enables KV caching. We visualize the attention mask of image tokens (Img1-2), prompt tokens (Pmt1-2), and text and mask tokens in the noise answer X_t (Ans1, [M], Ans3). Rows represent queries, while columns are keys. Colored squares indicate that queries and keys can interact.

where $p_\theta(X_0|I,P,X_t)$ factorizes into $\prod_{i=1}^{L} p_\theta(X_0^i|I,P,X_t)$ following the formulation in Section 2.2. Notably, the loss is only computed over mask tokens where $X_t^i = [M]$, because $p_\theta(X_0^i|I,P,X_t)$ is not dependent on θ when $X_t^i \neq [M]$.

Complementary Masking. Prior diffusion language models (e.g., LLaDa, Dream) apply a stochastic estimator to Equation 2, masking tokens independently across samples in a batch. However, for vision-language tasks, this leads to inefficiencies: (1) only ∼50% of tokens contribute to the loss on average, and (2) critical answer tokens—often short and sparse in vision tasks like VQA—may not be masked, resulting in misaligned gradients for the vision encoder. For example, in `"The answer is dog."` the key token `"dog"` might be unmasked in X_t and thus ignored in loss computation. To address this, we introduce complementary masking: for each sample, we generate two masked versions X_t and X_t^C with disjoint corrupted spans (e.g., one masks `"The [M] [M] dog ."`, the other `"[M] answer is [M] [M]"`, ensuring all tokens are eventually used in training and improving sample efficiency and gradient flow. When computing the loss over X_t and X_t^C, we copy the encoded vision embeddings to further boost training efficiency. This process is illustrated in Figure 3a.

3.3 Inference Algorithms

At inference time, we first create a sequence of L mask tokens as X_1, where L is the response generation length. Then we gradually unmask them through K discrete timestamps $t_1..t_K$, where $t_1 = 1$ and $t_K = 0$, until we reach a clean, mask-free sequence X_0. At each timestamp t_i, we sample a fully unmasked sequence through $p_\theta(X_0|X_{t_i})$ and re-mask $L \times t_{i+1}$ tokens to obtain $X_{t_{i+1}}$. Both L and K are hyperparameters for inference. Additionally, we define $\frac{K}{L}$ as "fraction of the number of functional evaluations (NFE)" to measure sample efficiency. For example, when NFE = 100%, the diffusion model generates one token per forward pass; at NFE = 50%, it generates an average of two tokens per forward pass. Overall, the inference process of LaViDa is similar to prior DMs such as LLaDa, with two key exceptions:

Prefix-DLM. While DLMs theoretically offer superior speed–quality tradeoffs at inference, they are often slower than AR models in practice because they cannot leverage KV caching [57]. This issue is particularly evident for multimodal prompts containing many visual tokens. To avoid recomputing keys and values for the visual embeddings and text prompts, we propose a novel Prefix-DLM scheme inspired by the autoregressive prefix-LM. Prefix-DLM adopts a specialized attention mask in which visual and prompt tokens can only attend to other visual and prompt tokens, while answer tokens can attend to all tokens. Figure 3b illustrates this setup. With this design, we can cache the keys and values of the visual and prompt tokens. Empirically, this leads to a speedup of up to 3.9× on COCO captioning tasks. Further details are provided in Section 4.5.

Schedule Shift. Diffusion language models (DLMs) allow trading speed for quality via the number of discretization steps K. Prior models like LLaDa and Dream use a linear schedule, unmasking $\frac{L}{K}$ tokens uniformly over $t \in [0, 1]$. However, we find this leads to performance degradation at low sampling steps. Inspired by SD3 [21], we adopt a shifting schedule:

$$t'_i = s_\alpha(t_i) = \frac{\alpha t_i}{1 + (\alpha - 1)t_i} \tag{3}$$

Here, $s_\alpha(t)$ is a monotonic map with $t_0 = t'_0 = 0$, $t_K = t'_K = 1$. When $\alpha < 1$ (we use $\alpha = \frac{1}{3}$), the schedule is convex—leading to more tokens being unmasked earlier. We found that this setup outperforms alternatives. Notably, this conclusion differs from that of continuous diffusion models like SD3 and previous masked diffusion models for image generation [11], which showed concave schedules ($\alpha > 1$) are more preferable. We ensure at least one token is unmasked per step. Further details are provided in Section 4 and Appendix A.2.

4 Experiments

4.1 Setup

At a high level, LaViDa employs a two-stage training process. In the pretraining phase (stage-1), only the projector is updated to align the visual embeddings with the latent space of the DLM. In the finetuning phase (stage-2), we jointly train all components end-to-end for instruction-following. Additionally, we further finetune the stage-2 model for additional steps and obtain two specialized models for reasoning and text-infilling tasks (LaViDa-Reason and LaViDa-FIM). We provide more details of these specialized models in Section 4.3 and 4.4. We use 558K image-text pairs as our stage-1 data, and 1M visual instruction-following examples as our stage-2 data. Further details on the dataset and training setup are provided in Appendix B.

We evaluate LaViDa on a wide range of vision-language tasks. Unless otherwise stated, we report results obtained using the stage-2 model with LLaDa-8B as the language backbone. We use `lmms-eval` package [83] for evaluation and set the sequence length L to be the maximum generation length used for evaluating AR models. We set $K = L$, or NFE=100% by default. Results under differet NFE are explored in Section 4.5 and Appendix B.3 and B.4.

4.2 Main Results

Table 1 reports the results of LaViDa using LLaDA-8B (LaViDa-L) and Dream-7B (LaViDa-D) as the language backbones on vision-understanding tasks. We compare with several open-source, open-data models with similar data sizes and parameter counts: LLaVa-1.6-7B [45, 43] and Open-LLaVa-Next-Llama3-8B [15]. We also include comparisons with frontier open-sourced models of similar size that are trained on larger datasets, namely LLaVa-OneVision-7B [36], Qwen2.5-VL-7B [5], and InternVL-38B [85].

LaViDa demonstrates competitive performance across a wide range of tasks spanning General, Reasoning, OCR, and Science categories. In general vision-language understanding, LaViDa-L achieves the highest score on MMMU [80] (43.3), outperforming all comparable models. LaViDa-D also ranks second on several benchmarks in this category. For reasoning tasks, both models surpass similarly scaled baselines on math-heavy and spatially grounded benchmarks. In Science, LaViDa achieves the best and second-best scores on ScienceQA [52] (81.4 and 80.2, respectively) while performing on par with Open-Llava-Next on AI2D [32], a complex diagram-based benchmark. Finally, in OCR LaViDa shows competitive performance but lags behind some of the latest AR models. This gap is primarily due to our use of average pooling for vision token compression, which leads to the loss of fine-grained spatial information. While this was a necessary trade-off given our limited compute budget, it poses challenges for tasks requiring precise text recognition and layout understanding. These results highlight the strength of LaViDa, demonstrating that diffusion-based approaches can scale competitively with AR models while achieving robust performance across a wide range of vision-language tasks.

Table 1: **LaViDa's Performance on Visual Understanding Tasks.** We report results on General, Reasoning, OCR, and Science Benchmarks. Dashes (–) denote results not reported. Open-Lnxt: Open-LLaVA-Next-Llama-3-8B; L-OV: LLaVA-OneVision-7B; Qwen2.5: Qwen2.5-VL-7B; Intern3: Intern-VL3-8B.

	LaViDa-L	**LaViDa-D**	**LLaVa-1.6**	**Open-Lnxt**	**L-OV**	**Qwen2.5**	**Intern3**
#Params	8B	7B	7B	8B	7B	7B	8B
#Images (Pretrain)	0.6M	0.6M	0.6M	0.6M	0.6M	>7M	-
#Images (SFT)	1.0M	1.0M	0.7M	1.0M	7.2M	∼2M	21.7M
			General				
MME-P [23]	1365.6	1463.5	1519.3	**1610.9**	1580.0	-	-
VQAv2 [24]	72.2	75.2	**80.1**	71.9	-	-	-
MMBench [47]	70.5	73.8	54.6	**74.4**	80.8	83.5	83.4
MMMU [80]	**43.3**	42.6	35.1	37.4	48.8	58.6	65.6
			Reasoning				
MME-C [23]	341.1	**378.9**	322.5	336.8	418.0	-	-
MathVista [51]	**44.8**	42.1	34.4	41.8	63.2	68.2	75.2
MathVerse [84]	**27.2**	24.1	14.3	14.6	-	-	-
MathVision [74]	**20.4**	19.4	12.8	14.1	-	-	-
			Science				
ScienceQA [52]	80.2	**81.4**	73.2	78.3	96.0	-	-
AI2D [32]	70.0	69.0	66.6	**70.2**	81.4	83.9	85.2
			OCR				
TextVQA [65]	56.3	57.1	**64.9**	61.7	-	84.9	80.2
DocVQA [55]	59.0	56.1	**74.4**	69.9	87.5	95.7	92.7
ChartQA [53]	64.6	61.0	54.8	**69.7**	80.0	87.3	86.6
InfoVQA [54]	34.2	36.2	**37.1**	36.7	68.8	82.6	76.8

Table 2: **Performance of Specialized stage-3 Models.** We report (a) performance of LaViDa-Reason on math reasoning tasks and (b) performance of LaViDa-FIM on constrained poem completion task.

(a) Math benchmark results after long CoT distillation.

	M.Vista↑	M.Verse↑	M.Vision↑
LaViDa	44.8	27.2	20.4
LaViDa -Reason	**45.2**	**29.3**	**24.0**
Rel. Δ	+1%	+8%	+18%

(b) Sentence and sample-level constraint satisfaction for poem completion tasks.

	Sentence↑	Sample↑
LaViDa	**1.00**	**1.00**
LaViDa-FIM	**1.00**	**1.00**
LLaVa-1.6-7B	0.41	0.37
Qwen2.5-VL-7B	0.45	0.16

4.3 Reasoning Distillation

Prior work has distilled LLMs [70] and VLMs [18, 73] using long chain-of-thought (CoT) data to elicit strong reasoning capabilities [25]. In the same spirit, we study the reasoning abilities of LaViDa by conducting additional stage-3 training using 19.2K CoT examples distilled from VL-Rethinker-7B, a strong reasoning model. We refer to the finetuned model as LaViDa-Reason. We evaluate it on MathVista [51], MathVerse [84], and MathVision [74] with CoT generation, comparing against the stage-2 results without CoT. We set the maximum generation length $L = 1024$ for these tasks. We report these results in Table 2a. We find that LaViDa-Reason outperforms LaViDa across all benchmarks, with the most significant gains observed on the most challenging MathVision reasoning dataset ($+18\%$ relative improvement). Further details are provided in Appendix B.3.

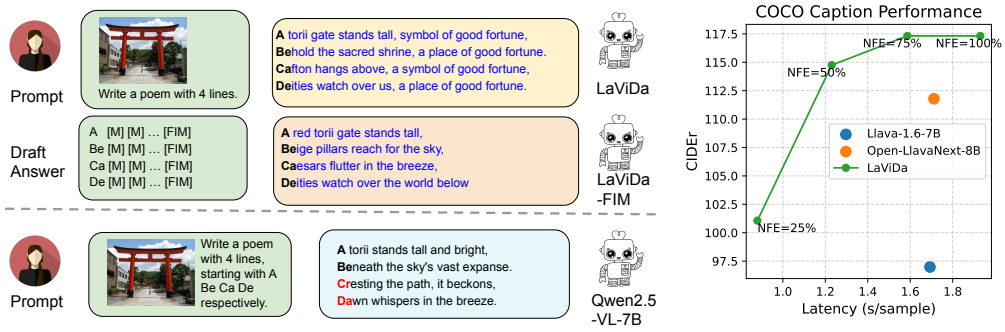

(a) Text-Infilling (b) Speed vs. Quality Tradeoff

Figure 4: **We showcase the advantages of LaViDa over AR VLMS in terms of controllability and speed.** (a) Qualitative comparison on constrained poem generation between LaViDa /LaViDa-FIM and AR models. LaViDa variants successfully satisfy line-level constraints and adapt token length per line, unlike AR baselines. (b) Speed–quality tradeoff for image captioning on COCO 2017. By adjusting the number of discretization steps (K), LaViDa offers a tunable balance between latency and output quality (CIDEr score).

4.4 Text Infilling

LaViDa offers strong controllability for text generation, particularly in text infilling. Given a draft of L tokens containing L_M masks, we jump to timestep $t = \frac{L_M}{L}$ and run standard inference to reach $t = 0$. This directly replaces L_M masks with L_M tokens. However, in practice, the intended completion may require fewer tokens—e.g., `"There is a [M] [M] [M] [M] in the image"` might become either `"dog"` or `"traffic light"`. To allow variable-length completions, we conduct an additional stage-3 training using a 20% subset of stage-2 data and refer to this model as LaViDa-FIM. During training, we insert random-length `[S] ... [S] [FIM]` sequences mid-text. At inference, we append `[FIM]` to masked segments (e.g., `[M] [M] [M] [M] [FIM]`) to signal flexible termination. The model can then generate completions like `[dog] [S] [S] [S] [FIM]` or `[traffic] [light] [S] [S] [FIM]`.

While FIM objectives are often discussed in the context of language tasks (e.g., code completion) [63, 7], they are equally relevant to multimodal applications. Figure 4a shows qualitative results on constrained poem generation, where the models generate a poem describing an image, with each line starting with specific syllables. Both LaViDa and LaViDa-FIM complete the task successfully, unlike AR models. Notably, LaViDa-FIM adapts token counts per line. Table 2b shows quantitative results over 100 samples: both LaViDa variants achieve 100% constraint satisfaction, while AR baselines remain below 50%. Additional results on other text-infilling use cases are provided in Appendix B.2.

4.5 Speed vs. Quality Trade Off

LaViDa offers a convenient way to achieve speed-quality tradeoffs by controlling the number of discretization steps K. We compare the performance on image captioning with 500 images from the COCO 2017 val dataset [42] with varying K. We set the maximum generation length to 32, and experimented with $K \in \{32, 24, 16, 8\}$, or equivalently, NFE$\in \{100\%, 75\%, 50\%, 25\%\}$. We report the average latency per image measured on a single A5000 GPU and the CIDEr score in Figure 4b. At NFE=100%, LaViDa achieves a higher CIDEr score than AR baselines but is slightly slower. At NFE=75% and NFE=50%, LaViDa is faster than the AR baselines and achieves better quality. At NFE=25%, it is significantly faster but trails in performance. This indicates that LaViDa can flexibly adjust its inference speed based on application needs—allowing users to trade off generation latency and output quality depending on their specific requirements.

Effect of KV Cache. The speed of LaViDa relies on our proposed Prefix-DLM setup, which allows us to cache the keys and values of visual and prompt tokens [3]. In Table 3a, we compare the speed and sample quality between the proposed Prefix-DLM step and the uncached full-attention-mask step used in prior works like LLaDa. We find that Prefix-DLM significantly reduces latency and achieves a maximum speedup of 3.9×, with marginal performance cost. These experiments are performed using our stage-2 model, which is trained on a full-attention mask. We discuss training with customized

masks and customized kernels in Appendix B.4. In short, we found that these alternatives lead to considerable training overhead while offering little benefit.

Table 3: **Speed-Quality Tradeoff.** (a) We compare COCO image captioning performance with and without Prefix-DLM caching. Latency is measured in seconds/sample. (b) We compare the performance of different schedules at different NFEs.

(a) Effect of KV Cache

Method	NFE	CIDEr ↑	Latency↓
Full-DLM	100%	**121.0**	7.65
Prefix-DLM	100%	117.3	1.93
Full-DLM	50%	118.6	4.13
Prefix-DLM	50%	114.8	**1.23**
Open-Lnxt-8B	–	111.8	1.71

(b) Effect of timestep shifting

	COCO Caption (CIDEr)↑			
NFE	25%	50%	75%	100%
cosine	87.7	102.2	110.8	117.3
linear	84.9	105.2	108.6	117.3
α=3	48.7	74.7	92.4	117.3
α=3^{-1}	**101.1**	**114.8**	**117.3**	**117.3**

Noise Schedule. To study the effect of the proposed time-step shifting schedule, we compare the performance of different schedules with NFE$\in \{100\%, 75\%, 50\%, 25\%\}$. We compare the proposed time-step shifting with $\alpha = 3$, and $\alpha = 3^{-1}$, as well as linear and cosine schedule baselines. We report results on COCO image captioning [42] in Table 3b. The convex schedule with $\alpha = 3^{-1}$ works the best. We also observe similar behaviors when conducting CoT inference using LaViDa-Reason on MathVision [74] dataset. At NFE=50%, $\alpha = 3^{-1}$ achieves an accuracy of 21.05, which is 30% higher than 16.12 achieved by a linear schedule. We provide results on MathVision in Appendix B.3.

4.6 Ablation Studies

We conducted a thorough ablation of various design choices. In the main paper, we discuss the effect of complementary masking and input image resolution. We provide further discussion of other design choices in the Appendix B.5. We conducted these experiments using a 200k subset of our (stage-2) training data. We report results in Tables 4a and 4b respectively. Table 4a shows that our proposed **complementary masking** scheme leads to considerable improvements across all benchmarks, most notably, complementary masking leads to a relative improvement of 67% on ScienceQA [52] with affordable compute overhead during the training (8% slowdown). Table 4b shows that **high-resolution input** improves overall performance, with the gain on OCR tasks being more pronounced than generic vision tasks (e.g., VQAv2). We did not use average pooling for the low-resolution setup. We provide additional details in the Appendix B.

Table 4: **Ablation Studies.** We study the effect of (a) complementary masking and (b) image resolution. For (a), we also report the wall clock time of 1000 training steps with a batch size of 128.

(a) Effect of complementary masking.

	w/o Comp.M.	w/ Comp.M.
MME↑	260.00	**297.00**
MathVista↑	28.40	**33.40**
ScienceQA↑	48.74	**81.49**
MMMU↑	38.56	**41.78**
Runtime↓	**8.2 hr**	8.9 hr

(b) Effect of image resolution.

	384^2	768^2
TextVQA↑	48.40	**55.65**
DocVQA↑	43.22	**58.72**
ChartQA↑	42.20	**57.70**
InfoVQA↑	26.48	**36.23**
VQAv2↑	65.92	**66.78**

5 Conclusion

In conclusion, we propose LaViDa, the first family of vision-language models based on DMs. To address various challenges, we introduce several novel training and inference techniques, including complementary masking, Prefix-DLM cache, and timestep shifting. Through extensive experiments, we show that these techniques significantly outperform a naive adaptation of DMs for visual tasks.

Using a comprehensive evaluation suite, we demonstrate that LaViDa achieves competitive performance compared to AR models trained under similar settings, while offering unique advantages such as speed–quality tradeoffs and controllability via text infilling. Our work proves that LaViDa can be a powerful alternative to exitsing AR VLMs, extending the prior success of DMs in the language domain to the vision space.

6 Acknowledgement

AG would like to acknowledge support from NSF CAREER Grant #2341040, Schmidt Sciences Early Career Fellowship, and Amazon Research Award.

References

[1] Jean-Baptiste Alayrac, Jeff Donahue, Pauline Luc, Antoine Miech, Iain Barr, Yana Hasson, Karel Lenc, Arthur Mensch, Katherine Millican, Malcolm Reynolds, et al. Flamingo: a visual language model for few-shot learning. *Advances in neural information processing systems*, 35:23716–23736, 2022.

[2] Anthropic. Claude 3.5 family. `https://www.anthropic.com/claude/sonnet`, 2024. Accessed: 2025-05-15.

[3] Marianne Arriola, Aaron Gokaslan, Justin T Chiu, Zhihan Yang, Zhixuan Qi, Jiaqi Han, Subham Sekhar Sahoo, and Volodymyr Kuleshov. Block diffusion: Interpolating between autoregressive and diffusion language models. *arXiv preprint arXiv:2503.09573*, 2025.

[4] Jacob Austin, Daniel D Johnson, Jonathan Ho, Daniel Tarlow, and Rianne Van Den Berg. Structured denoising diffusion models in discrete state-spaces. *Advances in neural information processing systems*, 34:17981–17993, 2021.

[5] Shuai Bai, Keqin Chen, Xuejing Liu, Jialin Wang, Wenbin Ge, Sibo Song, Kai Dang, Peng Wang, Shijie Wang, Jun Tang, et al. Qwen2. 5-vl technical report. *arXiv preprint arXiv:2502.13923*, 2025.

[6] Hritik Bansal, Arian Hosseini, Rishabh Agarwal, Vinh Q Tran, and Mehran Kazemi. Smaller, weaker, yet better: Training llm reasoners via compute-optimal sampling. *arXiv preprint arXiv:2408.16737*, 2024.

[7] Mohammad Bavarian, Heewoo Jun, Nikolas Tezak, John Schulman, Christine McLeavey, Jerry Tworek, and Mark Chen. Efficient training of language models to fill in the middle. *arXiv preprint arXiv:2207.14255*, 2022.

[8] Samy Bengio, Oriol Vinyals, Navdeep Jaitly, and Noam Shazeer. Scheduled sampling for sequence prediction with recurrent neural networks. *Advances in neural information processing systems*, 28, 2015.

[9] Daniele Rege Cambrin, Gabriele Scaffidi Militone, Luca Colomba, Giovanni Malnati, Daniele Apiletti, and Paolo Garza. Level up your tutorials: Vlms for game tutorials quality assessment. *arXiv preprint arXiv:2408.08396*, 2024.

[10] Huiwen Chang, Han Zhang, Jarred Barber, AJ Maschinot, Jose Lezama, Lu Jiang, Ming-Hsuan Yang, Kevin Murphy, William T Freeman, Michael Rubinstein, et al. Muse: Text-to-image generation via masked generative transformers. *arXiv preprint arXiv:2301.00704*, 2023.

[11] Huiwen Chang, Han Zhang, Lu Jiang, Ce Liu, and William T Freeman. Maskgit: Masked generative image transformer. In *Proceedings of the IEEE/CVF conference on computer vision and pattern recognition*, pages 11315–11325, 2022.

[12] Guiming Hardy Chen, Shunian Chen, Ruifei Zhang, Junying Chen, Xiangbo Wu, Zhiyi Zhang, Zhihong Chen, Jianquan Li, Xiang Wan, and Benyou Wang. Allava: Harnessing gpt4v-synthesized data for a lite vision-language model, 2024.

[13] Jiaqi Chen, Jianheng Tang, Jinghui Qin, Xiaodan Liang, Lingbo Liu, Eric P Xing, and Liang Lin. Geoqa: A geometric question answering benchmark towards multimodal numerical reasoning. *arXiv preprint arXiv:2105.14517*, 2021.

[14] Lin Chen, Jisong Li, Xiaoyi Dong, Pan Zhang, Conghui He, Jiaqi Wang, Feng Zhao, and Dahua Lin. Sharegpt4v: Improving large multi-modal models with better captions. *arXiv preprint arXiv:2311.12793*, 2023.

[15] Lin Chen and Long Xing. Open-llava-next: An open-source implementation of llava-next series for facilitating the large multi-modal model community. `https://github.com/xiaoachen98/Open-LLaVA-NeXT`, 2024.

[16] Zhe Chen, Weiyun Wang, Hao Tian, Shenglong Ye, Zhangwei Gao, Erfei Cui, Wenwen Tong, Kongzhi Hu, Jiapeng Luo, Zheng Ma, et al. How far are we to gpt-4v? closing the gap to commercial multimodal models with open-source suites. *Science China Information Sciences*, 67(12):220101, 2024.

[17] Zhe Chen, Jiannan Wu, Wenhai Wang, Weijie Su, Guo Chen, Sen Xing, Muyan Zhong, Qinglong Zhang, Xizhou Zhu, Lewei Lu, et al. Internvl: Scaling up vision foundation models and aligning for generic visual-linguistic tasks. In *Proceedings of the IEEE/CVF conference on computer vision and pattern recognition*, pages 24185–24198, 2024.

[18] Yihe Deng, Hritik Bansal, Fan Yin, Nanyun Peng, Wei Wang, and Kai-Wei Chang. Openvlthinker: An early exploration to complex vision-language reasoning via iterative self-improvement. *arXiv preprint arXiv:2503.17352*, 2025.

[19] Jacob Devlin, Ming-Wei Chang, Kenton Lee, and Kristina Toutanova. Bert: Pre-training of deep bidirectional transformers for language understanding. In *Proceedings of the 2019 conference of the North American chapter of the association for computational linguistics: human language technologies, volume 1 (long and short papers)*, pages 4171–4186, 2019.

[20] Juechu Dong, Boyuan Feng, Driss Guessous, Yanbo Liang, and Horace He. Flex attention: A programming model for generating optimized attention kernels. *arXiv preprint arXiv:2412.05496*, 2024.

[21] Patrick Esser, Sumith Kulal, Andreas Blattmann, Rahim Entezari, Jonas Müller, Harry Saini, Yam Levi, Dominik Lorenz, Axel Sauer, Frederic Boesel, et al. Scaling rectified flow transformers for high-resolution image synthesis. In *Forty-first international conference on machine learning*, 2024.

[22] Daniel Fried, Armen Aghajanyan, Jessy Lin, Sida Wang, Eric Wallace, Freda Shi, Ruiqi Zhong, Wen-tau Yih, Luke Zettlemoyer, and Mike Lewis. Incoder: A generative model for code infilling and synthesis. *arXiv preprint arXiv:2204.05999*, 2022.

[23] Chaoyou Fu, Peixian Chen, Yunhang Shen, Yulei Qin, Mengdan Zhang, Xu Lin, Jinrui Yang, Xiawu Zheng, Ke Li, Xing Sun, et al. Mme: A comprehensive evaluation benchmark for multimodal large language models. *arXiv preprint arXiv:2306.13394*, 2023.

[24] Yash Goyal, Tejas Khot, Douglas Summers-Stay, Dhruv Batra, and Devi Parikh. Making the V in VQA matter: Elevating the role of image understanding in Visual Question Answering. In *Conference on Computer Vision and Pattern Recognition (CVPR)*, 2017.

[25] Daya Guo, Dejian Yang, Haowei Zhang, Junxiao Song, Ruoyu Zhang, Runxin Xu, Qihao Zhu, Shirong Ma, Peiyi Wang, Xiao Bi, et al. Deepseek-r1: Incentivizing reasoning capability in llms via reinforcement learning. *arXiv preprint arXiv:2501.12948*, 2025.

[26] Zonghao Guo, Ruyi Xu, Yuan Yao, Junbo Cui, Zanlin Ni, Chunjiang Ge, Tat-Seng Chua, Zhiyuan Liu, and Gao Huang. Llava-uhd: an lmm perceiving any aspect ratio and high-resolution images. In *European Conference on Computer Vision*, pages 390–406. Springer, 2024.

[27] Kaiming He, Xinlei Chen, Saining Xie, Yanghao Li, Piotr Dollár, and Ross Girshick. Masked autoencoders are scalable vision learners. In *Proceedings of the IEEE/CVF conference on computer vision and pattern recognition*, pages 16000–16009, 2022.

[28] Cheng-Ping Hsieh, Simeng Sun, Samuel Kriman, Shantanu Acharya, Dima Rekesh, Fei Jia, Yang Zhang, and Boris Ginsburg. Ruler: What's the real context size of your long-context language models? *arXiv preprint arXiv:2404.06654*, 2024.

[29] Minghui Hu, Chuanxia Zheng, Heliang Zheng, Tat-Jen Cham, Chaoyue Wang, Zuopeng Yang, Dacheng Tao, and Ponnuthurai N Suganthan. Unified discrete diffusion for simultaneous vision-language generation. *arXiv*, 2022.

[30] Drew A Hudson and Christopher D Manning. Gqa: A new dataset for real-world visual reasoning and compositional question answering. In *Proceedings of the IEEE/CVF conference on computer vision and pattern recognition*, pages 6700–6709, 2019.

[31] Kushal Kafle, Brian Price, Scott Cohen, and Christopher Kanan. Dvqa: Understanding data visualizations via question answering. In *Proceedings of the IEEE conference on computer vision and pattern recognition*, pages 5648–5656, 2018.

[32] Aniruddha Kembhavi, Mike Salvato, Eric Kolve, Minjoon Seo, Hannaneh Hajishirzi, and Ali Farhadi. A diagram is worth a dozen images. In *Computer Vision–ECCV 2016: 14th European Conference, Amsterdam, The Netherlands, October 11–14, 2016, Proceedings, Part IV 14*, pages 235–251. Springer, 2016.

[33] Geewook Kim, Teakgyu Hong, Moonbin Yim, JeongYeon Nam, Jinyoung Park, Jinyeong Yim, Wonseok Hwang, Sangdoo Yun, Dongyoon Han, and Seunghyun Park. Ocr-free document understanding transformer. In *European Conference on Computer Vision (ECCV)*, 2022.

[34] Alexander Kirillov, Eric Mintun, Nikhila Ravi, Hanzi Mao, Chloe Rolland, Laura Gustafson, Tete Xiao, Spencer Whitehead, Alexander C Berg, Wan-Yen Lo, et al. Segment anything. In *Proceedings of the IEEE/CVF international conference on computer vision*, pages 4015–4026, 2023.

[35] Ranjay Krishna, Yuke Zhu, Oliver Groth, Justin Johnson, Kenji Hata, Joshua Kravitz, Stephanie Chen, Yannis Kalantidis, Li-Jia Li, David A Shamma, et al. Visual genome: Connecting language and vision using crowdsourced dense image annotations. *International journal of computer vision*, 123:32–73, 2017.

[36] Bo Li, Yuanhan Zhang, Dong Guo, Renrui Zhang, Feng Li, Hao Zhang, Kaichen Zhang, Peiyuan Zhang, Yanwei Li, Ziwei Liu, et al. Llava-onevision: Easy visual task transfer. *arXiv preprint arXiv:2408.03326*, 2024.

[37] Chunyuan Li, Zhe Gan, Zhengyuan Yang, Jianwei Yang, Linjie Li, Lijuan Wang, Jianfeng Gao, et al. Multimodal foundation models: From specialists to general-purpose assistants. *Foundations and Trends® in Computer Graphics and Vision*, 16(1-2):1–214, 2024.

[38] Shufan Li, Konstantinos Kallidromitis, Akash Gokul, Zichun Liao, Yusuke Kato, Kazuki Kozuka, and Aditya Grover. Omniflow: Any-to-any generation with multi-modal rectified flows. *arXiv preprint arXiv:2412.01169*, 2024.

[39] Xiang Li, John Thickstun, Ishaan Gulrajani, Percy S Liang, and Tatsunori B Hashimoto. Diffusion-lm improves controllable text generation. *Advances in neural information processing systems*, 35:4328–4343, 2022.

[40] Xiaobo Liang, Zecheng Tang, Juntao Li, and Min Zhang. Open-ended long text generation via masked language modeling. In *Proceedings of the 61st Annual Meeting of the Association for Computational Linguistics (Volume 1: Long Papers)*, pages 223–241, 2023.

[41] Ji Lin, Hongxu Yin, Wei Ping, Pavlo Molchanov, Mohammad Shoeybi, and Song Han. Vila: On pre-training for visual language models. In *Proceedings of the IEEE/CVF conference on computer vision and pattern recognition*, pages 26689–26699, 2024.

[42] Tsung-Yi Lin, Michael Maire, Serge Belongie, James Hays, Pietro Perona, Deva Ramanan, Piotr Dollár, and C Lawrence Zitnick. Microsoft coco: Common objects in context. In *Computer vision–ECCV 2014: 13th European conference, zurich, Switzerland, September 6-12, 2014, proceedings, part v 13*, pages 740–755. Springer, 2014.

[43] Haotian Liu. Llava v1.6 vicuna-7b. `https://huggingface.co/liuhaotian/llava-v1.6-vicuna-7b`, 2023. Accessed: 2025-05-14.

[44] Haotian Liu, Chunyuan Li, Yuheng Li, and Yong Jae Lee. Improved baselines with visual instruction tuning. In *Proceedings of the IEEE/CVF Conference on Computer Vision and Pattern Recognition*, pages 26296–26306, 2024.

[45] Haotian Liu, Chunyuan Li, Yuheng Li, Bo Li, Yuanhan Zhang, Sheng Shen, and Yong Jae Lee. Llava-next: Improved reasoning, ocr, and world knowledge, January 2024.

[46] Haotian Liu, Chunyuan Li, Qingyang Wu, and Yong Jae Lee. Visual instruction tuning. *Advances in neural information processing systems*, 36:34892–34916, 2023.

[47] Yuan Liu, Haodong Duan, Yuanhan Zhang, Bo Li, Songyang Zhang, Wangbo Zhao, Yike Yuan, Jiaqi Wang, Conghui He, Ziwei Liu, et al. Mmbench: Is your multi-modal model an all-around player? In *European conference on computer vision*, pages 216–233. Springer, 2024.

[48] Zhijian Liu, Ligeng Zhu, Baifeng Shi, Zhuoyang Zhang, Yuming Lou, Shang Yang, Haocheng Xi, Shiyi Cao, Yuxian Gu, Dacheng Li, et al. Nvila: Efficient frontier visual language models. *arXiv preprint arXiv:2412.04468*, 2024.

[49] Aaron Lou, Chenlin Meng, and Stefano Ermon. Discrete diffusion modeling by estimating the ratios of the data distribution. *arXiv preprint arXiv:2310.16834*, 2023.

[50] Justin Lovelace, Varsha Kishore, Chao Wan, Eliot Shekhtman, and Kilian Q Weinberger. Latent diffusion for language generation. *Advances in Neural Information Processing Systems*, 36:56998–57025, 2023.

[51] Pan Lu, Hritik Bansal, Tony Xia, Jiacheng Liu, Chunyuan Li, Hannaneh Hajishirzi, Hao Cheng, Kai-Wei Chang, Michel Galley, and Jianfeng Gao. Mathvista: Evaluating mathematical reasoning of foundation models in visual contexts. *arXiv preprint arXiv:2310.02255*, 2023.

[52] Pan Lu, Swaroop Mishra, Tony Xia, Liang Qiu, Kai-Wei Chang, Song-Chun Zhu, Oyvind Tafjord, Peter Clark, and Ashwin Kalyan. Learn to explain: Multimodal reasoning via thought chains for science question answering. In *The 36th Conference on Neural Information Processing Systems (NeurIPS)*, 2022.

[53] Ahmed Masry, Do Long, Jia Qing Tan, Shafiq Joty, and Enamul Hoque. ChartQA: A benchmark for question answering about charts with visual and logical reasoning. In *Findings of the Association for Computational Linguistics: ACL 2022*, pages 2263–2279, Dublin, Ireland, May 2022. Association for Computational Linguistics.

[54] Minesh Mathew, Viraj Bagal, Rubèn Tito, Dimosthenis Karatzas, Ernest Valveny, and CV Jawahar. Infographicvqa. In *Proceedings of the IEEE/CVF Winter Conference on Applications of Computer Vision*, pages 1697–1706, 2022.

[55] Minesh Mathew, Dimosthenis Karatzas, and CV Jawahar. Docvqa: A dataset for vqa on document images. In *Proceedings of the IEEE/CVF winter conference on applications of computer vision*, pages 2200–2209, 2021.

[56] Anand Mishra, Shashank Shekhar, Ajeet Kumar Singh, and Anirban Chakraborty. Ocr-vqa: Visual question answering by reading text in images. In *ICDAR*, 2019.

[57] Shen Nie, Fengqi Zhu, Zebin You, Xiaolu Zhang, Jingyang Ou, Jun Hu, Jun Zhou, Yankai Lin, Ji-Rong Wen, and Chongxuan Li. Large language diffusion models. *arXiv preprint arXiv:2502.09992*, 2025.

[58] OpenAI. Gpt-4o system card. *arXiv preprint arXiv:2410.21276*, 2024.

[59] Dustin Podell, Zion English, Kyle Lacey, Andreas Blattmann, Tim Dockhorn, Jonas Müller, Joe Penna, and Robin Rombach. Sdxl: Improving latent diffusion models for high-resolution image synthesis. *arXiv preprint arXiv:2307.01952*, 2023.

[60] Alec Radford, Jong Wook Kim, Chris Hallacy, Aditya Ramesh, Gabriel Goh, Sandhini Agarwal, Girish Sastry, Amanda Askell, Pamela Mishkin, Jack Clark, et al. Learning transferable visual models from natural language supervision. In *International conference on machine learning*, pages 8748–8763. PmLR, 2021.

[61] Colin Raffel, Noam Shazeer, Adam Roberts, Katherine Lee, Sharan Narang, Michael Matena, Yanqi Zhou, Wei Li, and Peter J Liu. Exploring the limits of transfer learning with a unified text-to-text transformer. *Journal of machine learning research*, 21(140):1–67, 2020.

[62] Robin Rombach, Andreas Blattmann, Dominik Lorenz, Patrick Esser, and Björn Ommer. High-resolution image synthesis with latent diffusion models. In *Proceedings of the IEEE/CVF conference on computer vision and pattern recognition*, pages 10684–10695, 2022.

[63] Baptiste Roziere, Jonas Gehring, Fabian Gloeckle, Sten Sootla, Itai Gat, Xiaoqing Ellen Tan, Yossi Adi, Jingyu Liu, Romain Sauvestre, Tal Remez, et al. Code llama: Open foundation models for code. *arXiv preprint arXiv:2308.12950*, 2023.

[64] Subham Sahoo, Marianne Arriola, Yair Schiff, Aaron Gokaslan, Edgar Marroquin, Justin Chiu, Alexander Rush, and Volodymyr Kuleshov. Simple and effective masked diffusion language models. *Advances in Neural Information Processing Systems*, 37:130136–130184, 2024.

[65] Amanpreet Singh, Vivek Natarjan, Meet Shah, Yu Jiang, Xinlei Chen, Devi Parikh, and Marcus Rohrbach. Towards vqa models that can read. In *Proceedings of the IEEE Conference on Computer Vision and Pattern Recognition*, pages 8317–8326, 2019.

[66] Alexander Swerdlow, Mihir Prabhudesai, Siddharth Gandhi, Deepak Pathak, and Katerina Fragkiadaki. Unified multimodal discrete diffusion. *arXiv preprint arXiv:2503.20853*, 2025.

[67] Wei Ren Tan, Chee Seng Chan, Hernan Aguirre, and Kiyoshi Tanaka. Improved artgan for conditional synthesis of natural image and artwork. *IEEE Transactions on Image Processing*, 28(1):394–409, 2019.

[68] Zineng Tang, Ziyi Yang, Chenguang Zhu, Michael Zeng, and Mohit Bansal. Any-to-any generation via composable diffusion. *Advances in Neural Information Processing Systems*, 36:16083–16099, 2023.

[69] Gemini Team, Petko Georgiev, Ving Ian Lei, Ryan Burnell, Libin Bai, Anmol Gulati, Garrett Tanzer, Damien Vincent, Zhufeng Pan, Shibo Wang, et al. Gemini 1.5: Unlocking multimodal understanding across millions of tokens of context. *arXiv preprint arXiv:2403.05530*, 2024.

[70] OpenThoughts Team. Open Thoughts. https://open-thoughts.ai, January 2025.

[71] Ashish Vaswani, Noam Shazeer, Niki Parmar, Jakob Uszkoreit, Llion Jones, Aidan N Gomez, Łukasz Kaiser, and Illia Polosukhin. Attention is all you need. *Advances in neural information processing systems*, 30, 2017.

[72] Changyuan Wang, Ziwei Wang, Xiuwei Xu, Yansong Tang, Jie Zhou, and Jiwen Lu. Q-vlm: Post-training quantization for large vision-language models. *arXiv preprint arXiv:2410.08119*, 2024.

[73] Haozhe Wang, Chao Qu, Zuming Huang, Wei Chu, Fangzhen Lin, and Wenhu Chen. Vl-rethinker: Incentivizing self-reflection of vision-language models with reinforcement learning. *arXiv preprint arXiv:2504.08837*, 2025.

[74] Ke Wang, Junting Pan, Weikang Shi, Zimu Lu, Houxing Ren, Aojun Zhou, Mingjie Zhan, and Hongsheng Li. Measuring multimodal mathematical reasoning with math-vision dataset. In *The Thirty-eight Conference on Neural Information Processing Systems Datasets and Benchmarks Track*, 2024.

[75] Peng Wang, Shuai Bai, Sinan Tan, Shijie Wang, Zhihao Fan, Jinze Bai, Keqin Chen, Xuejing Liu, Jialin Wang, Wenbin Ge, et al. Qwen2-vl: Enhancing vision-language model's perception of the world at any resolution. *arXiv preprint arXiv:2409.12191*, 2024.

[76] Hu Xu, Saining Xie, Xiaoqing Ellen Tan, Po-Yao Huang, Russell Howes, Vasu Sharma, Shang-Wen Li, Gargi Ghosh, Luke Zettlemoyer, and Christoph Feichtenhofer. Demystifying clip data. *arXiv preprint arXiv:2309.16671*, 2023.

[77] Chenyu Yang, Xuan Dong, Xizhou Zhu, Weijie Su, Jiahao Wang, Hao Tian, Zhe Chen, Wenhai Wang, Lewei Lu, and Jifeng Dai. Pvc: Progressive visual token compression for unified image and video processing in large vision-language models. *arXiv preprint arXiv:2412.09613*, 2024.

[78] Ling Yang, Ye Tian, Bowen Li, Xinchen Zhang, Ke Shen, Yunhai Tong, and Mengdi Wang. Multimodal large diffusion language models. *arXiv preprint arXiv:2505.15809*, 2025.

[79] Jiacheng Ye, Zhihui Xie, Lin Zheng, Jiahui Gao, Zirui Wu, Xin Jiang, Zhenguo Li, and Lingpeng Kong. Dream 7b, 2025.

[80] Xiang Yue, Yuansheng Ni, Kai Zhang, Tianyu Zheng, Ruoqi Liu, Ge Zhang, Samuel Stevens, Dongfu Jiang, Weiming Ren, Yuxuan Sun, Cong Wei, Botao Yu, Ruibin Yuan, Renliang Sun, Ming Yin, Boyuan Zheng, Zhenzhu Yang, Yibo Liu, Wenhao Huang, Huan Sun, Yu Su, and Wenhu Chen. Mmmu: A massive multi-discipline multimodal understanding and reasoning benchmark for expert agi. In *Proceedings of CVPR*, 2024.

[81] Eric Zelikman, Yuhuai Wu, Jesse Mu, and Noah Goodman. Star: Bootstrapping reasoning with reasoning. *Advances in Neural Information Processing Systems*, 35:15476–15488, 2022.

[82] Xiaohua Zhai, Basil Mustafa, Alexander Kolesnikov, and Lucas Beyer. Sigmoid loss for language image pre-training. In *Proceedings of the IEEE/CVF international conference on computer vision*, pages 11975–11986, 2023.

[83] Kaichen Zhang, Bo Li, Peiyuan Zhang, Fanyi Pu, Joshua Adrian Cahyono, Kairui Hu, Shuai Liu, Yuanhan Zhang, Jingkang Yang, Chunyuan Li, and Ziwei Liu. Lmms-eval: Reality check on the evaluation of large multimodal models, 2024.

[84] Renrui Zhang, Dongzhi Jiang, Yichi Zhang, Haokun Lin, Ziyu Guo, Pengshuo Qiu, Aojun Zhou, Pan Lu, Kai-Wei Chang, Peng Gao, et al. Mathverse: Does your multi-modal llm truly see the diagrams in visual math problems? *arXiv preprint arXiv:2403.14624*, 2024.

[85] Jinguo Zhu, Weiyun Wang, Zhe Chen, Zhaoyang Liu, Shenglong Ye, Lixin Gu, Yuchen Duan, Hao Tian, Weijie Su, Jie Shao, et al. Internvl3: Exploring advanced training and test-time recipes for open-source multimodal models. *arXiv preprint arXiv:2504.10479*, 2025.

[86] Alon Ziv, Itai Gat, Gael Le Lan, Tal Remez, Felix Kreuk, Alexandre Défossez, Jade Copet, Gabriel Synnaeve, and Yossi Adi. Masked audio generation using a single non-autoregressive transformer. *arXiv preprint arXiv:2401.04577*, 2024.

NeurIPS Paper Checklist

1. **Claims**

   Question: Do the main claims made in the abstract and introduction accurately reflect the paper's contributions and scope?

   Answer: [Yes]

   Justification: The abstract and introduction highlight three contributions. Our main contribution is the proposal DM-based VLMs. Our claims of competitive performance is supported by the experimental results in Section 4.

   Guidelines:

   - The answer NA means that the abstract and introduction do not include the claims made in the paper.
   - The abstract and/or introduction should clearly state the claims made, including the contributions made in the paper and important assumptions and limitations. A No or NA answer to this question will not be perceived well by the reviewers.
   - The claims made should match theoretical and experimental results, and reflect how much the results can be expected to generalize to other settings.
   - It is fine to include aspirational goals as motivation as long as it is clear that these goals are not attained by the paper.

2. **Limitations**

   Question: Does the paper discuss the limitations of the work performed by the authors?

   Answer: [Yes]

   Justification: We provide discussions of limitation in Appendix D.

   Guidelines:

   - The answer NA means that the paper has no limitation while the answer No means that the paper has limitations, but those are not discussed in the paper.
   - The authors are encouraged to create a separate "Limitations" section in their paper.
   - The paper should point out any strong assumptions and how robust the results are to violations of these assumptions (e.g., independence assumptions, noiseless settings, model well-specification, asymptotic approximations only holding locally). The authors should reflect on how these assumptions might be violated in practice and what the implications would be.
   - The authors should reflect on the scope of the claims made, e.g., if the approach was only tested on a few datasets or with a few runs. In general, empirical results often depend on implicit assumptions, which should be articulated.
   - The authors should reflect on the factors that influence the performance of the approach. For example, a facial recognition algorithm may perform poorly when image resolution is low or images are taken in low lighting. Or a speech-to-text system might not be used reliably to provide closed captions for online lectures because it fails to handle technical jargon.
   - The authors should discuss the computational efficiency of the proposed algorithms and how they scale with dataset size.
   - If applicable, the authors should discuss possible limitations of their approach to address problems of privacy and fairness.
   - While the authors might fear that complete honesty about limitations might be used by reviewers as grounds for rejection, a worse outcome might be that reviewers discover limitations that aren't acknowledged in the paper. The authors should use their best judgment and recognize that individual actions in favor of transparency play an important role in developing norms that preserve the integrity of the community. Reviewers will be specifically instructed to not penalize honesty concerning limitations.

3. **Theory assumptions and proofs**

   Question: For each theoretical result, does the paper provide the full set of assumptions and a complete (and correct) proof?

Answer: [NA]

Justification: We do not include theoretical results.

Guidelines:

- The answer NA means that the paper does not include theoretical results.
- All the theorems, formulas, and proofs in the paper should be numbered and cross-referenced.
- All assumptions should be clearly stated or referenced in the statement of any theorems.
- The proofs can either appear in the main paper or the supplemental material, but if they appear in the supplemental material, the authors are encouraged to provide a short proof sketch to provide intuition.
- Inversely, any informal proof provided in the core of the paper should be complemented by formal proofs provided in appendix or supplemental material.
- Theorems and Lemmas that the proof relies upon should be properly referenced.

4. **Experimental result reproducibility**

   Question: Does the paper fully disclose all the information needed to reproduce the main experimental results of the paper to the extent that it affects the main claims and/or conclusions of the paper (regardless of whether the code and data are provided or not)?

   Answer: [Yes]

   Justification: Experiment details are provided in Section 4.1 and Appendix B

   Guidelines:

   - The answer NA means that the paper does not include experiments.
   - If the paper includes experiments, a No answer to this question will not be perceived well by the reviewers: Making the paper reproducible is important, regardless of whether the code and data are provided or not.
   - If the contribution is a dataset and/or model, the authors should describe the steps taken to make their results reproducible or verifiable.
   - Depending on the contribution, reproducibility can be accomplished in various ways. For example, if the contribution is a novel architecture, describing the architecture fully might suffice, or if the contribution is a specific model and empirical evaluation, it may be necessary to either make it possible for others to replicate the model with the same dataset, or provide access to the model. In general. releasing code and data is often one good way to accomplish this, but reproducibility can also be provided via detailed instructions for how to replicate the results, access to a hosted model (e.g., in the case of a large language model), releasing of a model checkpoint, or other means that are appropriate to the research performed.
   - While NeurIPS does not require releasing code, the conference does require all submissions to provide some reasonable avenue for reproducibility, which may depend on the nature of the contribution. For example
     (a) If the contribution is primarily a new algorithm, the paper should make it clear how to reproduce that algorithm.
     (b) If the contribution is primarily a new model architecture, the paper should describe the architecture clearly and fully.
     (c) If the contribution is a new model (e.g., a large language model), then there should either be a way to access this model for reproducing the results or a way to reproduce the model (e.g., with an open-source dataset or instructions for how to construct the dataset).
     (d) We recognize that reproducibility may be tricky in some cases, in which case authors are welcome to describe the particular way they provide for reproducibility. In the case of closed-source models, it may be that access to the model is limited in some way (e.g., to registered users), but it should be possible for other researchers to have some path to reproducing or verifying the results.

5. **Open access to data and code**

Question: Does the paper provide open access to the data and code, with sufficient instructions to faithfully reproduce the main experimental results, as described in supplemental material?

Answer: [No]

Justification: We will provide open access to the data and code in camera ready version. See our reproducibility statement in Appendix **??**.

Guidelines:

- The answer NA means that paper does not include experiments requiring code.
- Please see the NeurIPS code and data submission guidelines (`https://nips.cc/public/guides/CodeSubmissionPolicy`) for more details.
- While we encourage the release of code and data, we understand that this might not be possible, so "No" is an acceptable answer. Papers cannot be rejected simply for not including code, unless this is central to the contribution (e.g., for a new open-source benchmark).
- The instructions should contain the exact command and environment needed to run to reproduce the results. See the NeurIPS code and data submission guidelines (`https://nips.cc/public/guides/CodeSubmissionPolicy`) for more details.
- The authors should provide instructions on data access and preparation, including how to access the raw data, preprocessed data, intermediate data, and generated data, etc.
- The authors should provide scripts to reproduce all experimental results for the new proposed method and baselines. If only a subset of experiments are reproducible, they should state which ones are omitted from the script and why.
- At submission time, to preserve anonymity, the authors should release anonymized versions (if applicable).
- Providing as much information as possible in supplemental material (appended to the paper) is recommended, but including URLs to data and code is permitted.

6. **Experimental setting/details**

   Question: Does the paper specify all the training and test details (e.g., data splits, hyperparameters, how they were chosen, type of optimizer, etc.) necessary to understand the results?

   Answer: [Yes]

   Justification: They are documented in Section 4.1 and Appendix B.

   Guidelines:

   - The answer NA means that the paper does not include experiments.
   - The experimental setting should be presented in the core of the paper to a level of detail that is necessary to appreciate the results and make sense of them.
   - The full details can be provided either with the code, in appendix, or as supplemental material.

7. **Experiment statistical significance**

   Question: Does the paper report error bars suitably and correctly defined or other appropriate information about the statistical significance of the experiments?

   Answer: [No]

   Justification: We follow the standard procedure of reporting VLM evaluations, which generally do not include error bars. Conducting multiple experiment runs with different random seeds is also very expensive. However, because of the large size of evaluation data, reported results should be considered as significant.

   Guidelines:

   - The answer NA means that the paper does not include experiments.
   - The authors should answer "Yes" if the results are accompanied by error bars, confidence intervals, or statistical significance tests, at least for the experiments that support the main claims of the paper.

- The factors of variability that the error bars are capturing should be clearly stated (for example, train/test split, initialization, random drawing of some parameter, or overall run with given experimental conditions).
- The method for calculating the error bars should be explained (closed form formula, call to a library function, bootstrap, etc.)
- The assumptions made should be given (e.g., Normally distributed errors).
- It should be clear whether the error bar is the standard deviation or the standard error of the mean.
- It is OK to report 1-sigma error bars, but one should state it. The authors should preferably report a 2-sigma error bar than state that they have a 96% CI, if the hypothesis of Normality of errors is not verified.
- For asymmetric distributions, the authors should be careful not to show in tables or figures symmetric error bars that would yield results that are out of range (e.g. negative error rates).
- If error bars are reported in tables or plots, The authors should explain in the text how they were calculated and reference the corresponding figures or tables in the text.

8. **Experiments compute resources**

   Question: For each experiment, does the paper provide sufficient information on the computer resources (type of compute workers, memory, time of execution) needed to reproduce the experiments?

   Answer: [Yes]

   Justification: These are detailed in Appendix B.

   Guidelines:

   - The answer NA means that the paper does not include experiments.
   - The paper should indicate the type of compute workers CPU or GPU, internal cluster, or cloud provider, including relevant memory and storage.
   - The paper should provide the amount of compute required for each of the individual experimental runs as well as estimate the total compute.
   - The paper should disclose whether the full research project required more compute than the experiments reported in the paper (e.g., preliminary or failed experiments that didn't make it into the paper).

9. **Code of ethics**

   Question: Does the research conducted in the paper conform, in every respect, with the NeurIPS Code of Ethics `https://neurips.cc/public/EthicsGuidelines`?

   Answer: [Yes]

   Justification: We follow the code of ethics.

   Guidelines:

   - The answer NA means that the authors have not reviewed the NeurIPS Code of Ethics.
   - If the authors answer No, they should explain the special circumstances that require a deviation from the Code of Ethics.
   - The authors should make sure to preserve anonymity (e.g., if there is a special consideration due to laws or regulations in their jurisdiction).

10. **Broader impacts**

    Question: Does the paper discuss both potential positive societal impacts and negative societal impacts of the work performed?

    Answer: [Yes]

    Justification: Appendix E.

    Guidelines:

    - The answer NA means that there is no societal impact of the work performed.
    - If the authors answer NA or No, they should explain why their work has no societal impact or why the paper does not address societal impact.

- Examples of negative societal impacts include potential malicious or unintended uses (e.g., disinformation, generating fake profiles, surveillance), fairness considerations (e.g., deployment of technologies that could make decisions that unfairly impact specific groups), privacy considerations, and security considerations.
- The conference expects that many papers will be foundational research and not tied to particular applications, let alone deployments. However, if there is a direct path to any negative applications, the authors should point it out. For example, it is legitimate to point out that an improvement in the quality of generative models could be used to generate deepfakes for disinformation. On the other hand, it is not needed to point out that a generic algorithm for optimizing neural networks could enable people to train models that generate Deepfakes faster.
- The authors should consider possible harms that could arise when the technology is being used as intended and functioning correctly, harms that could arise when the technology is being used as intended but gives incorrect results, and harms following from (intentional or unintentional) misuse of the technology.
- If there are negative societal impacts, the authors could also discuss possible mitigation strategies (e.g., gated release of models, providing defenses in addition to attacks, mechanisms for monitoring misuse, mechanisms to monitor how a system learns from feedback over time, improving the efficiency and accessibility of ML).

11. **Safeguards**

    Question: Does the paper describe safeguards that have been put in place for responsible release of data or models that have a high risk for misuse (e.g., pretrained language models, image generators, or scraped datasets)?

    Answer: [Yes]

    Justification: Appendix E.

    Guidelines:

    - The answer NA means that the paper poses no such risks.
    - Released models that have a high risk for misuse or dual-use should be released with necessary safeguards to allow for controlled use of the model, for example by requiring that users adhere to usage guidelines or restrictions to access the model or implementing safety filters.
    - Datasets that have been scraped from the Internet could pose safety risks. The authors should describe how they avoided releasing unsafe images.
    - We recognize that providing effective safeguards is challenging, and many papers do not require this, but we encourage authors to take this into account and make a best faith effort.

12. **Licenses for existing assets**

    Question: Are the creators or original owners of assets (e.g., code, data, models), used in the paper, properly credited and are the license and terms of use explicitly mentioned and properly respected?

    Answer: [Yes]

    Justification: Appendix F

    Guidelines:

    - The answer NA means that the paper does not use existing assets.
    - The authors should cite the original paper that produced the code package or dataset.
    - The authors should state which version of the asset is used and, if possible, include a URL.
    - The name of the license (e.g., CC-BY 4.0) should be included for each asset.
    - For scraped data from a particular source (e.g., website), the copyright and terms of service of that source should be provided.
    - If assets are released, the license, copyright information, and terms of use in the package should be provided. For popular datasets, `paperswithcode.com/datasets` has curated licenses for some datasets. Their licensing guide can help determine the license of a dataset.

- For existing datasets that are re-packaged, both the original license and the license of the derived asset (if it has changed) should be provided.
- If this information is not available online, the authors are encouraged to reach out to the asset's creators.

13. **New assets**

    Question: Are new assets introduced in the paper well documented and is the documentation provided alongside the assets?

    Answer: [NA]

    Justification: No asset released at the time of submission.

    Guidelines:

    - The answer NA means that the paper does not release new assets.
    - Researchers should communicate the details of the dataset/code/model as part of their submissions via structured templates. This includes details about training, license, limitations, etc.
    - The paper should discuss whether and how consent was obtained from people whose asset is used.
    - At submission time, remember to anonymize your assets (if applicable). You can either create an anonymized URL or include an anonymized zip file.

14. **Crowdsourcing and research with human subjects**

    Question: For crowdsourcing experiments and research with human subjects, does the paper include the full text of instructions given to participants and screenshots, if applicable, as well as details about compensation (if any)?

    Answer: [NA]

    Justification: not used.

    Guidelines:

    - The answer NA means that the paper does not involve crowdsourcing nor research with human subjects.
    - Including this information in the supplemental material is fine, but if the main contribution of the paper involves human subjects, then as much detail as possible should be included in the main paper.
    - According to the NeurIPS Code of Ethics, workers involved in data collection, curation, or other labor should be paid at least the minimum wage in the country of the data collector.

15. **Institutional review board (IRB) approvals or equivalent for research with human subjects**

    Question: Does the paper describe potential risks incurred by study participants, whether such risks were disclosed to the subjects, and whether Institutional Review Board (IRB) approvals (or an equivalent approval/review based on the requirements of your country or institution) were obtained?

    Answer: [NA]

    Justification: The paper does not involve crowdsourcing nor research with human subjects.

    Guidelines:

    - The answer NA means that the paper does not involve crowdsourcing nor research with human subjects.
    - Depending on the country in which research is conducted, IRB approval (or equivalent) may be required for any human subjects research. If you obtained IRB approval, you should clearly state this in the paper.
    - We recognize that the procedures for this may vary significantly between institutions and locations, and we expect authors to adhere to the NeurIPS Code of Ethics and the guidelines for their institution.
    - For initial submissions, do not include any information that would break anonymity (if applicable), such as the institution conducting the review.

16. **Declaration of LLM usage**

Question: Does the paper describe the usage of LLMs if it is an important, original, or non-standard component of the core methods in this research? Note that if the LLM is used only for writing, editing, or formatting purposes and does not impact the core methodology, scientific rigorousness, or originality of the research, declaration is not required.

Answer: [Yes]

Justification: See Appendix G. We use open-sourced LLMs to generate some reasoning data. The result is fully reproducible. We did not using any close-sourced LLMs.

Guidelines:

- The answer NA means that the core method development in this research does not involve LLMs as any important, original, or non-standard components.
- Please refer to our LLM policy (`https://neurips.cc/Conferences/2025/LLM`) for what should or should not be described.

A Additional Technical Details

A.1 Formulation of Discrete Diffusion Models (DMs)

In this section, we provide a detailed review of the formulation of Discrete Diffusion Models (DMs) briefly described in 2.2. Given a text sequence of L tokens $X_0 = [X_0^1, X_0^2, ...X_0^L]$, the forward process $q(X_t|X_s)$ gradually coverts it to a sequence of mask tokens $[M]$, denoted by $X_1 = [X_1^1, X_1^2, ...X_1^L]$ over the continuous time-interval $[0, 1]$, with $1 \geq t \geq s \geq 0$. Formally, this process is defined as

$$q(X_t^i|X_s^i) = \begin{cases} \text{Cat}(X_t^i; \mathbf{M}), & \text{if } X_s^i = M \\ \text{Cat}(X_t^i; \frac{1-t}{1-s}\mathbf{X_s^i} + \frac{t-s}{1-s}\mathbf{M}), & \text{if } X_s^i \neq M \end{cases} \tag{4}$$

which has the marginal

$$q(X_t^i|X_0^i) = \text{Cat}(X_t^i; (1-t)\mathbf{X_0^i} + t\mathbf{M}) \tag{5}$$

where $\text{Cat}(.)$ denotes a categorical distribution and $\mathbf{M}, \mathbf{X_0^i}, \mathbf{X_s^i}$ are probability vectors. MDLM [64] showed that the posterior of the reversal process $p(X_s|X_t, X_0)$ can be simplified into the following

$$p(X_s^i|X_t^i, X_0^i) = \begin{cases} \text{Cat}(X_s^i; \mathbf{X_t^i}), & \text{if } X_s^i \neq M \\ \text{Cat}(X_t^i; \frac{t-s}{t}\mathbf{X_0^i} + \frac{s}{t}\mathbf{M}), & \text{if } X_s^i = M \end{cases} \tag{6}$$

In practice, we use the categorical distribution induced by the neural network's prediction $p_\theta(X_0^i|X_t)$ in place of $\mathbf{X_0^i}$ the sample from the reverse process, which gives the following parametrization

$$p_\theta(X_s^i|X_t) = \begin{cases} \text{Cat}(X_s^i; \mathbf{X_t^i}), & \text{if } X_s^i \neq M \\ \text{Cat}(X_t^i; \frac{t-s}{t}p_\theta(X_0^i|X_t) + \frac{s}{t}\mathbf{M}), & \text{if } X_s^i = M \end{cases} \tag{7}$$

Inference Algorithm. Given a target length L and discretization steps $t_0, t_1...t_K$ where $t_0 = 0$ and $t_K = 1$, we first initialize $X_{t_K}^{1:L} = X_1^{1:L} = M$, then use Equation 7 to repetitively sample $p_\theta(X_{t_{k-1}}|X_{t_k})$ until we reach $t_0 = 0$. In this process, we also assume $p_\theta(X_{t_{k-1}}|X_{t_k})$ factorize into $\prod_{i=1}^L p_\theta(X_{t_{k-1}}^i|X_{t_k})$ following previous works [57, 64, 49].

Training Objective. Recall that the training objective of DMs introduced in Section 2.2 is formulated as

$$\mathcal{L}_{\text{DLM}} = -\mathbb{E}_{t,X_0,X_t}\left[\frac{1}{t}\log p_\theta(X_0|X_t)\right] \tag{8}$$

where $p_\theta(X_0|X_t)$ factorizes into $\prod_{i=1}^L p_\theta(X_0^i|X_t)$. However, Equation 6 shows that $p_\theta(X_0^i|X_t)$ has a closed form solution that depends only on X_t when $X_t^i \neq M$. Intuitively, this comes from the fact that in the reverse process, once a token X_i changes from a mask token to a clean text token, it stays the same thereafter. Based on this observation, we can remove the terms that does not depend on the neural network θ from the learning objective, giving us the following loss

$$\mathcal{L}_{\text{DLM}} = -\mathbb{E}_{t,X_0,X_t}\left[\frac{1}{t}\sum_{X_t^i \neq M}\log p_\theta(X_0^i|X_t)\right] \tag{9}$$

Hence, the loss is only computed over the masked indices in X_t.

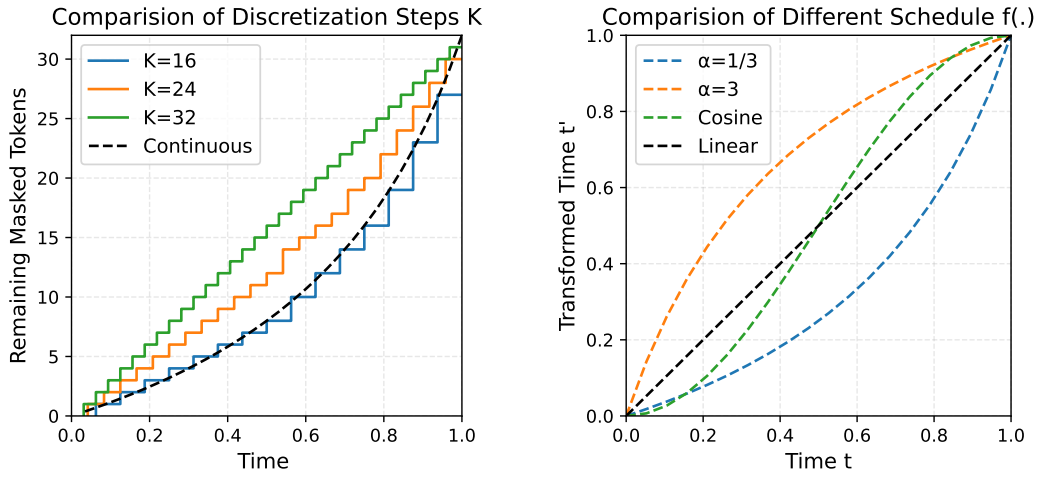

(a) Discretized Schedules at Different K.

(b) Different Choice of Continuous Schedules f.

Figure 5: **Visualization of Schedules** (a) We visualize discretization results of the same continuous schedule (dashed line) under different numbers of sampling steps $K \in \{16, 24, 32\}$ at $L = 32$. (b) We visualize various choices of continuous schedules: Shift($\alpha = 3^{-1}$), Shift($\alpha = 3$), Cosine, and Linear.

A.2 Timestep shifting Schedule

Given a sequence of L tokens, and a timestep $t \in [0, 1]$, in expectation X_t contains tL masked tokens. In practice, we implement Equation 7 such that there are exactly $\lfloor tL \rfloor$ masked tokens and $L - \lfloor tL \rfloor$ clean text tokens at timestep t during the sampling process.

Given a fixed number of sampling step K, we define the canonical discretization as $t_i = \frac{i}{K}$ for $i = 0, 1..K$, with $t_0 = 0$ and $t_1 = 1$. This forms a uniformed sampling schedule, where roughly a fixed mount of $\frac{L}{K}$ tokens is unmakes at each sampling step. Any other schedule t'_i can be defined as $t'_i = f(t_i)$ where $f(.)$ is a monotonic function such that $f(0) = 0$ and $f(1) = 1$.

When $f(.)$ is convex, the slope will be steeper when t get closer to 1 , indicating that more tokens are decoded in earlier sampling steps. By contrast, when $f(.)$ is concave, the slope will be steeper when t get closer to 0, indicating that more tokens are decoded in later sampling steps.

Choice of Schedule. We explored a wide range of choices for the continuous schedule $f(.)$. The *timestep shifting schedule* is a family of schedule defined as

$$f(t) = s_\alpha(t) = \frac{\alpha t}{1 + (\alpha - 1)t} \tag{10}$$

where α is a hyperparameter. When $\alpha < 1$, the schedule is convex. When $\alpha > 1$, the schedule is concave. The *cosine schedule* is defined as

$$f(t) = 1 - \frac{1}{2}(1 + \cos(\pi t)) \tag{11}$$

The *linear schedule* is just the identity function $f(t) = t$. We visualize these choices in Figure 5b.

Rounding in Discretization. In principle, we can pick any $f(.)$. However, given a particular choice of L and K, if $\lfloor f(t_k)L \rfloor$ and $\lfloor f(t_{k-1})L \rfloor$ yields the same integer, then no tokens are unmasked when we compute $p_\theta(X_{t_{k-1}}|X_{t_k})$. Hence, the actual number of function calls to the model θ may be less than, K depending on the choice of $f(.)$. To make the sampling compute cost more predictable and allow for a fair comparison across different schedulers, we augment all choices of $f(.)$ to $f^K(.)$ such that $\lfloor f^K(t_{k-1})L \rfloor < \lfloor f^K(t_k)L \rfloor$ (i.e. at least one token is decoded at each step). Note that in the sampling process, the exact real value of $f^K(t_k)$ does not matter as long as it does not change

$\lfloor f^K(t_k)L \rfloor$. Hence, we can parameterize the sampling process in an alternative manner using a sequence of integers $F_k^K = \lfloor f^K(t_k)L \rfloor$, with $F_0^K = 0$ and $F_1^K = L$. Formally, we set F^K by solving the following optimization objective

$$\begin{aligned} \min_{\{F_{0:K}^K\} \subset \{0,1..L\}} \quad & \sum_{k=0}^{K} \left\| F_k^K - f(t_k)L \right\|^2 \\ \text{subject to} \quad & F_{k-1} < F_k, \quad \text{for } k = 1, 2, \ldots, K \\ & F_0^K = 0 \\ & F_1^K = L \end{aligned}$$

We visualize such examples in Figure 5a. We set $L = 32$ and $K \in \{16, 24, 32\}$. When $K = 32$, F^K is effectively a linear schedule, since the only schedule with 32 steps that satisfy the constraint $F_{k-1} < F_k$ is a uniform schedule where we unmask exactly one token per step. As K reduces to 24 and 16, we see the discretized schedule becomes closer to the continuous scheduler (visualized in dashed line).

A.3 Padding

We follow the design of LLaDa [57] and apply the loss function to both standard text tokens and padding tokens. AR models typically do not compute the loss over padding tokens. However, when sampling from DMs, we have a specified generation length L. In the generation process, we unmask L mask tokens to L non-mask tokens. Since the length of the desired answer may not be exactly L tokens, the model will generate padding tokens. To achieve this capability, we pad the sequences during the training, and apply the loss on the padding tokens following LLaDa.

B Additional Experiment Details and Results

B.1 Setup

In this section, we document the detailed training setup, including data, hyperparameters and compute used for the main experiments. Additional details about Prefix-DLM Cache can be found in B.4. Additional details about stage-3 math reasoning experiments can be found in B.3.

Training Data Composition. For the pretraining phase, we use LCS-558K [46] consists of 558K image-text pairs. For the finetuning phase, we mostly use the dataset released by Open-LLaVa-Next [15]. We made some small adjustments to the weight of each data source and increased the weight of some QA dataset. This is used to compensate the fact that our model only learns from a randomly chosen round at each training step for multi-round QA data. We document the precise dataset composition of our stage-2 training in Table 5.

Table 5: **Compositio of Stage-2 Training Data**. We report the data sources and sample sizes used to compose the Stage-2 finetuning data.

Data Source	Size	Data Source	Size	Data Source	Size
COCO[42]	349,860	GQA[30]	72,140	DocVQA[55]	10,211
ALLaVA-VFLAN[12]	202,966	Synthdog-En[33]	29,765	DVQA[31]	10,000
Visual Genome[35]	86,417	TextVQA[56]	21,953	SA-1B[34]	8,997
OCR VQA[56]	80,000	ChartQA [53]	18,317	LLaVA-150K [46]	2,988
GeoQA+ [13]	72,318	AI2D[32]	12,413	WikiArt[67]	500
Share-TextVQA [14]	500	Web-Celebrity[15]	500	Web-Landmark[15]	500

Training Hyperparameters. We use AdamW optimizer with a learning rate of 5e-3 with a cosine decay schedule for all experiments. For pretraining (Stage 1), we adopted a global batch size of 256 and trained for 1 epoch. For finetuning (Stage 2), we adopted a global batch size of 512 and trained for two epochs.

Compute Used. We used a mixture of A100s and A6000s for training experiments and A5000 for evaluations and inference speed benchmarks. Because of the memory constraint, we set the per GPU batch size to 8 on A100s and 4 on A6000s. We adjust the gradient accumulation steps accordingly so that the global batch size is always 256 for the pretraining and 128 for the finetuning stage.

Evaluation Setup. We implement our evlaution using `LMMS-Eval` [83] library. We use the default prompt provided by the library for all benchmarks. We report the split used and the generation length L in Table 6.

Table 6: **Evaluation Setup.** We report evaluation split and generation length L used to produce results of Table 1 in the main paper. *We use a generation length of 100 for LaViDa and a generation length of 1024 for LaViDa-Reason.

Dataset	Split	L	Dataset	Split	L
MME-P	test	100	MathVista*	testmini_format	100
VQAv2	val	16	MathVerse*	testmini_vision_dominant	100
MMBench	dev	100	MathVision*	mathvision_testmini	100
MMMU	val	16	ScienceQA	scienceqa-full	16
MME-C	test	16	AI2D	test	16
TextVQA	val	16	ChartQA	test	16
DocVQA	test	32	InfoVQA	test	32

B.2 Text-Infilling

In this section, we provide additional qualitative results of the text-infilling capability of LaViDa. We visualize the results in Figure 6. In the first example, we ask the model to extract multiple attributes from the image in JSON format. In the second example, we ask the model to edit a sentence based on the image. This is achieved by deleting the original sentence and inserting mask tokens. In the final example, we ask the model to complete a movie script based on the image prompt. LaViDa was able to successfully complete these tasks.

While it may be possible to achieve similar results using an AR model, they require careful prompting. By contrast, as shown in Figure 6, using a diffusion model for text-infilling is more straightfoward.

B.3 Math Reasoning

In this section, we provide additional training setup for LaViDa-Reason and provide additional experiment results on the speed-quality tradeoff on math reasoning.

Data and Training Setup. In §4.3, we train LaViDaon long chain-of-thought (CoT) data to get LaViDa-Reason. Specifically, we choose a strong 7B reasoning model, VLRethinker-7B [73] as a teacher model to generate the long reasoning traces. Further, we choose their own ViRL-39K data that contains (image, question, final answer). Subsequently, we generate the CoT and predicted final answer from the teacher model and filter the ones that lead to the correct final answer [81, 6]. This led to the creation of the final dataset of size $19.2K$.[1] In particular, we finetune LaViDaon this data for 5 epochs using the identical training setup as stage-2 (e.g., batch size, learning rates) and chose the checkpoint that achieves the best performance on MathVision (testmini). We observe that the same checkpoint achieved a good performance on the MathVerse and MathVista dataset too. During inference, we set the generation length to 1024 since LaViDa-Reason synthesizes long chain-of-thoughts for problem-solving.

Speed-Quality Tradeoff. In the main paper, we reported the speed-quality tradeoff results on COCO image captioning and discovered that the convex schedule works the best. We conducted similar study on LaViDa-Reason for CoT inference on MathVision dataset. We report these results in Table 7. Overall, the conclusion on CoT math reasoning task is similar to that on image captioning task, with the convex schedule performing the best across different choices of sampling steps. To

[1]We will release this data in the camera-ready version.

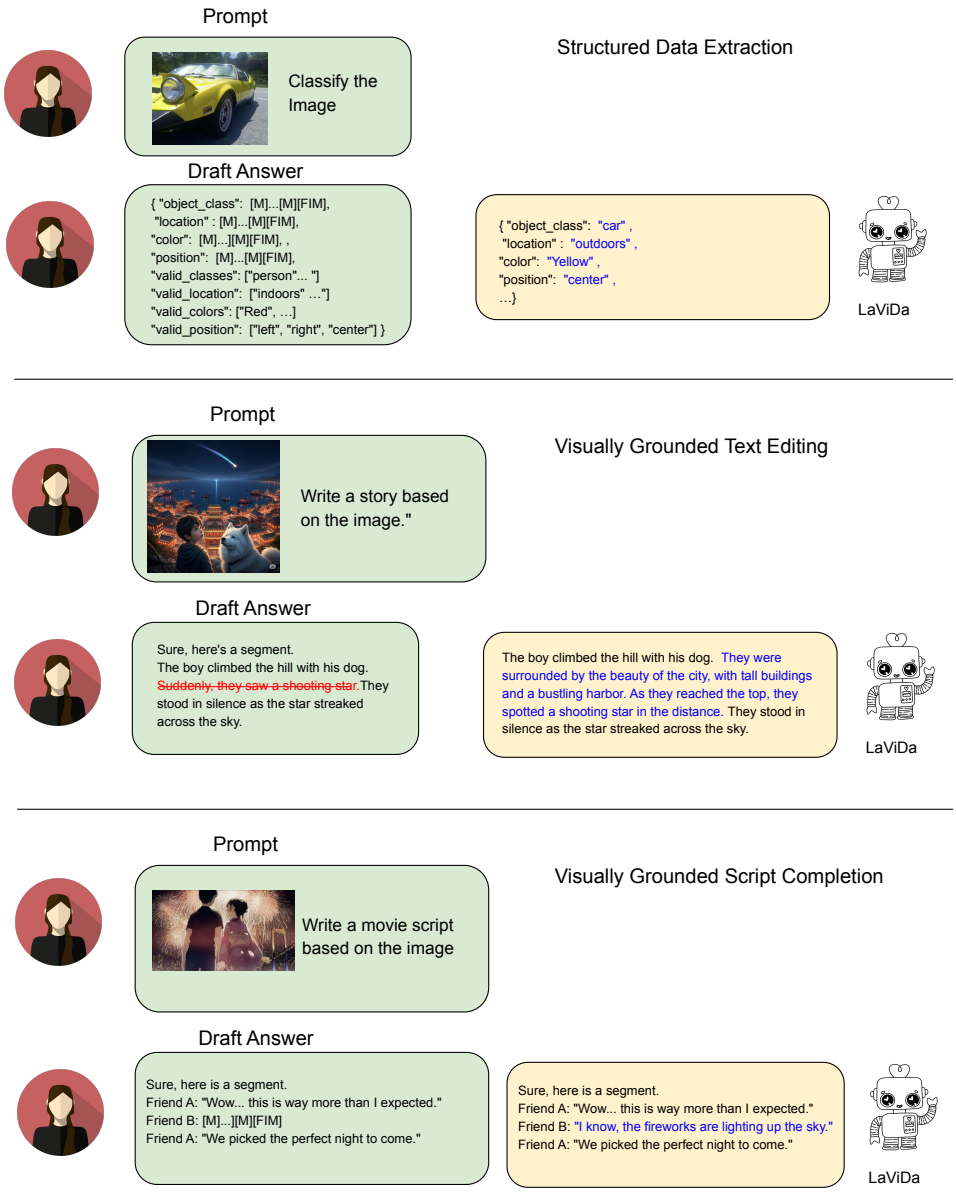

Figure 6: **Additional Qualitative Results for Text Infilling.** We showcase several useful applications of text-infilling capabilities.

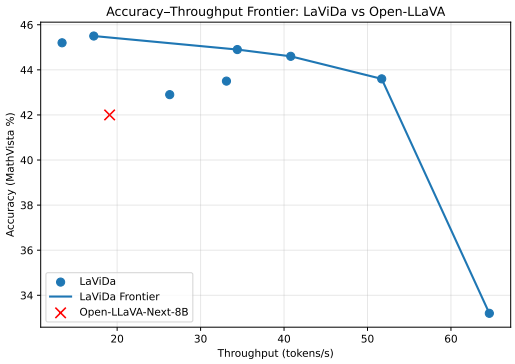

Figure 7: **Speed-Quality Tradeoff on MathVista Dataset.** We report the throughput and accuracy on MathVista dataset of LaViDa under a variety of inference setup.

further examine the speed-quality tradeoff, we visualize the inference throughput (tokens/s) and accuracy on MathVista dataset under different inference setup in Figure 7 and compare with Open-LLaVA-Next-8B baseline. LaViDa's frontier strictly dominates the performance of autoregressive Open-LLaVA-Next-8B both in terms of speed and quality.

Table 7: **Effect of different schedule on MathVision dataset.** We study the effect of different schedules on MathVision dataset using Chain-of-Though inference with LaViDa-Reason.

	MathVision Acc↑		
NFE	25% (256 steps)	50% (512 steps)	100% (1024 steps)
cosine	8.55	13.49	24.02
linear	10.86	16.12	24.02
α=3	5.59	8.88	24.02
α=3^{-1}	**12.5**	**21.05**	**24.02**

B.4 Prefix-DLM

In this section, we discuss several alternatives to our prefix-DLM setup that we explored and document the experiment results.

Inference Algorithm. Autoregressive models employ a causal attention mask. Because of this, they can leverage KV cache for effective inference. By contrast, discrete diffusion models (DMs) used a full attention mask. While DMs can decode multiple tokens in parallel, it cannot leverage attention mask for fast inference. Prefix-DLM combine the best of both worlds by introducing a prefix attention mask such that the queries of image embeddings and text prompts can only interact with keys and values of image embeddings and text prompts, but not the keys and values of answer tokens. Through this mechanism, we can leverage the KV cache for the image embeddings and text prompts. In vision-language applications with a long context (900+ vision tokens per image), this saves a lot of compute at inference time, while preserving the full bidirectional context.

A alternative to our prefix-DLM was the recently proposed semi-autoregressive Block-Diffusion [3], which uses a block-wise causal attention mask. In this setup, the input sequece are chunked into a sequence of fixed length blocks, each containing L_B tokens. A token in Block i can see all tokens in the past and current Block j with $j \leq i$, but cannot see all future blocks Block j with $j > i$. While this design allows it to leverage block-wise KV cache, it limits the bi-directional context to at most L_B tokens in the future, which is undesirable for tasks like text-infilling. Additionally, because of its semi-autoregressive nature, when we are generating Block i, we must see all mask-free past Blocks j with $j < i$. Hence, the naive training algorithm can mask at most L_B tokens in each training sample (i.e. the last block), which is inefficient. To address this issue, a customized attention kernel was developed to allow for parallel training. However, this leads to considerable training overhead. By contrast, Prefix-DLM can leverage the KV cache while having the full bidirectional context. It also

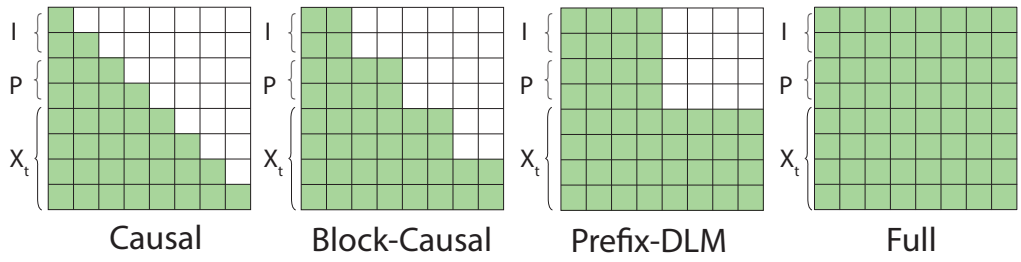

Figure 8: **Visualization of Different Choices of Attention Mask at Inference Time.** I represents the image embeddings, P represents the prompt tokens, and X_t represents the partially masked answer tokens. Each row represents a query and each column represents a key. Colored region indicts tokens queries and keys can interact with each other.

does not require any specialized training algorithms, since we adopt it as a pure inference technique of DMs.

We visualize the different choices of attention masks in Figure 8. We also compare the properties of different choices in 8.

Table 8: **Comparison of Different Choices of Attention Mask**. We compare properties of different choices of attention masks. The desired properties are highlighted.

Method	Attn. Mask	Bi-Direction Context	KV Cache	Training Overhead
AR	Causal	None	Yes	No
DM	Full	Full Seq.	No	No
Block-Diffusion	Block-Causal	Within Block	Yes	Yes
LaViDa	Prefix-DLM	Full Seq.	Yes	No

Training Algorithm. We adopt Prefix-DLM as a pure inference algorithm. Our training process is identical to that of a standard DM with full attention mask. We made this choice mostly because of efficiency reasons. We also explored adopting the prefix-DLM attention mask during the training (Prefix-DLM-FT) with four different but equivalent implementations. Generally, these four implementations are categorized into two classes: Prefix-DLM-FT1 and Prefix-DLM-FT2. We visualize these setups in Figure 9.

Recall from Section 3.2 that we adopted a complementary masking scheme, wherein given each triplet of image I, prompt P and answer X, we create two versions of partially masked answer X_t and X_t^C with complementary masking in order to utilize all tokens in the clean answer X. Empirically, this is achieved by copying the prompt embedding and concatenate X_t and X_t^C to different copies respectively (Left Column of Figure 9). By default, we use the full attention for both copies. We can adopt the Prefix-DLM attention mask during the training for each copy individually. We call this setup Prefix-DLM-FT1 (Middle Column of Figure 9). Alternatively, we can concatenate I, P, X_t, X_t^C into a single long sequence and manipulate the attention mask such that queries of I, P can see keys of I, P, queries of X_t can see keys of I, P, X_t and queries of X_t^C can see keys of I, P, X_t^C. We call this setup Prefix-DLM-FT2 (Right Column of Figure 9).

For each of the two variant Prefix-DLM-FT1 and Prefix-DLM-FT2, we designed two concrete implementations. The first set of implementations (Prefix-DLM-FT1-Mask,Prefix-DLM-FT2-Mask) simply construct a 2D attention mask of size $L \times L$ for each sample, where L is the sequence length, and pass it to the torch SDPA kernel. The second variant (Prefix-DLM-FT1-Flex,Prefix-DLM-FT2-Flex) merely constructs an integer tensor of size 3 per sample, containing the length of I, P, X. We then use a customized `flex_attention` module [20] to implement the attention mask implicitly based on the length of I, P, X.

Notably, these four variants of Prefix-DLM-FT generates identical loss value and will produce exactly the same training dynamics (disregarding small numerical differences between implementations). The only difference is the efficiency. Hence, we only benchmarked the performance and performed the full training using the most efficient version.

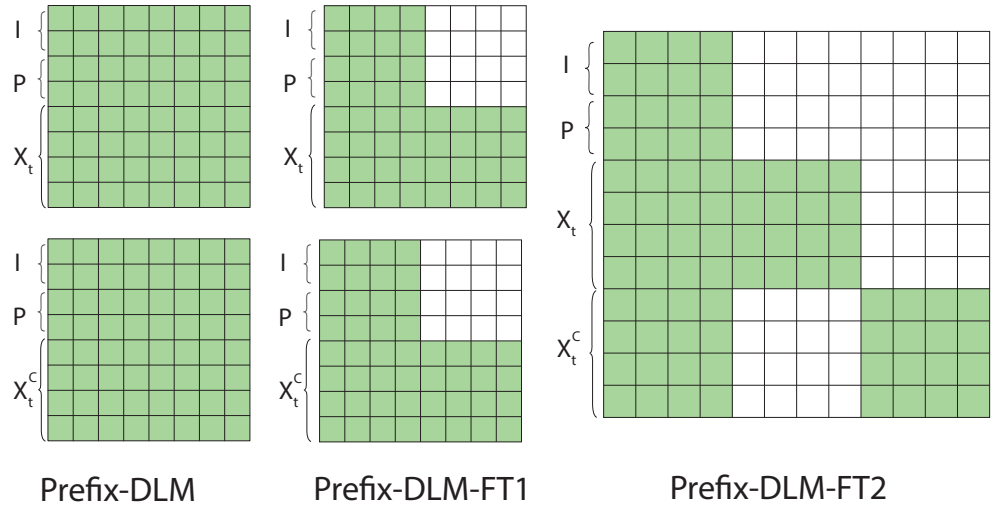

Figure 9: **Visualization of Training Strategies for Prefix-DLM.** Given each triplet of image I, prompt P and answer X, we create two versions of partially masked answer X_t and X_t^C with complementary masking.(Left) By default, we construct two sequence and apply full attention mask. (Middle) Prefix-DLM-FT1 applies prefix attention mask to each copy independently. (Right) Prefix-DLM-FT2 combines I, P, X_t, X_t^C into a single sequence and manipulate the attention mask to achieve an equivalent effect to Prefix-DLM-FT1.

We report the speed benchmark in Table 7. Overall, even the fastest finetuning version is 62% slower than the full attention mask baseline, suggesting a high overhead caused by batch-dependent masking strategies during training. We also report the model performance after 1,500 training steps (roughly 200k samples from the training data) in Table 10.

Overall, Prefix-DLM and Prefix-DLM-FT has mostly identical performance, with Prefix-DLM having a small lead over many tasks. Because of this, we consider the 62% overhead as unacceptable and opt for a training procedure using the full attention mask. This also gives user an additional dimension for speed-quality tradeoff: they can disable Prefix-DLM cache and use the full attention mask at inference to achieve a slightly better performance (Results shown in Table 3a in main paper).

Table 9: **Training Speed of Different Variants of Prefix-DLM.** We report the average training speed of different setup with a batch size of 128 on 8 A6000 GPUs.

Method	Speed(s/training step)
Prefix-DLM	**37.2**
Prefix-DLM-FT1-Mask	67.3
Prefix-DLM-FT2-Mask	82.6
Prefix-DLM-FT1-Kernel	60.2
Prefix-DLM-FT2-Kernel	74.4

Table 10: **Performance of Prefix-DLM and Prefix-DLM-FT across benchmarks.** We compare the performance of two variants after 1,500 steps of training.

	MMMU	VQAv2	MME	M.Vista	M.Verse	ScienceQA	AI2D
Prefix-DLM	**40.56**	**63.26**	286.79	33.60	**19.67**	**80.36**	**64.31**
Prefix-DLM-FT	40.10	61.02	**290.71**	**35.00**	18.15	80.15	64.15

Table 11: **Ablation Studies on the Choice of Vision Encoders.** We compare the performance of models with different vision encoders after 1,500 steps of training. On Average, SigLip improves over CLIP by **+1.86** and improves over MetaCLIP by **+2.77**.

	MMMU	VQAv2	MME	M.Vista	M.Verse	ScienceQA	AI2D
SigLip	**40.56**	**63.26**	286.79	33.60	19.67	**80.36**	**64.31**
CLIP	40.44	59.58	**288.21**	30.90	**20.05**	76.56	59.78
MetaCLIP	40.33	55.96	280.36	**33.80**	17.26	78.66	62.79

B.5 Ablation Studies

We conduct additional ablation studies over the choice of vision encoders. We experimented with SigLip[82], CLIP [60], and MetaCLIP[76]. We report the model performance after 1,500 training steps (roughly 200k samples from the training data) in Table 11. Overall, SigLip achieves the strongest overall performance, with notably gains in VQAv2, ScienceQA, and AI2D.

B.6 Additional Scaling

While LaViDa outperforms AR VLMs under comparable data scale, there is still a considerable gap between LaViDa and state-of-the-art AR VLMs. To validate the scalability of LaViDa, we scale the training schedule by 2x, resulting in considerable performance on general understanding and OCR tasks. We report these results in Table 12. Due to compute constraints, we left further scaling to future works.

Table 12: **Additional Scaling Experiments on OCR and General Understanding Tasks.**

Model	**MME**	**MMBench**	**ChartQA**	**DocVQA**	**InfoVQA**
LaViDa	341.1	70.5	64.6	59.0	34.2
+Additional Training	**444.3**	**75.6**	**74.9**	**68.6**	**43.4**
Open-LLaVA-Next-8B	336.8	74.4	69.7	69.9	36.7

C Additional Backgrounds

In this section, we provide additional discussions with relevant works not covered in the main paper.

Masked Generative Models. Masked generative modeling has a long history before the recent advancements of DMs. Earliest works such as BERT[19] and MAE[27] adopt the masked generative modeling objective as a pretraining objective to learn rich text and vision features. They mainly concern the utility of learnt features to downstream perception and understanding tasks, instead of the generation capability of the model. A series of subsequent works use mask modeling to build generative models for images [11, 10], texts [40] and audio [86]. Compared with these early works relying on ad-hoc sampler designs, recent works on DMs [49, 64] provided a principled way for training and sampling from masked generative models.

Multi-Modal Diffusion Models. Several works have explored to build a multi-modal diffsion models with vision-language capabilities. CoDi [68] and OmniFlow [38] build continuous diffusion model over a latent text embedding space and use autoregressive decoder to decode the generated latent mebeddings to actual texts. UniD3 [29] and UniDisc [66] build discrete diffusion models for simultaneous text and image generation. Overall, these models have limited language generation capabilities. Their experiments on text generations are limited in scale and mostly focusing on captioning. They cannot perform more complex instruction-following and understanding tasks (e.g. reasoning) like many modern autoregressive VLMs.

D Limitations

In this section, we discuss the limitations of LaViDa. There are mainly two limitations.

Scale. While LaViDaachieves competitive results when compared against similar-sized AR VLMs trained on a similar scale of data, there remain a considerable gap between LaViDa's performance and that of state-of-the-art open sourced VLMs such as LLaVa-OneVision and Qwen2.5-VL. These models either comes with more training data or larger model sizes. Future work should study if DMs scale well with a larger model and more training data.

OCR. LaViDa's performance on OCR tasks are slightly worse than the baselines, this can be mainly attributed to the average pooling operation which we introduced to reduce the sequence length by compressing the visual information. Concretely, LLaVa-1.6-7B and Open-LLaVa-Next-Llama3-8B baseline do not adopt average pooling, and uses 2880 tokens ($24 \times 24 \times 5$ Views) to represent each image. In our setup, removing the average pooling would lead to a total of 3645 tokens ($24 \times 24 \times 5$ Views) per image. Average pooling is necessary because the base model LLaDa and Dream has a context length of 4096 and 2048 respectively. Without average pooling, LLaDa will not have enough context length to fit longer training samples, while Dream will not have enough context length to even fit one image.

We also tried to extend the context length of these models via techniques such as rope rescaling, but achieved limited success. We experimented with extending Dream to 4096 context length and evaluate the model using the needle-in-a-haystack task [28] at 4096 context length. We found that Dream-7B (72.4 Acc) performs worse than LLaDa-8B (91.6 Acc) and Llama-3-8B (95.4 Acc).

We hope future works on DMs with longer context will provide stronger base models to finetune on vision-language applications.

E Boarder Impacts and Safeguards

Our model may inherit the biases embedded in the base model LLaDa-8B and Dream-7B, as well as biases incorporated in the training data. Our model may also suffer from the same hallucination problem as the base model. Just as any LLMs and VLMs, there is also the risk that our model is used to generate harmful or offensive content. Overall, our model is intended to be used by researchers to build a strong diffusion model for vision-language applications. We do not recommend it be used for any other purposes.

F License Information for Data and Models

We report the licenses of the used artifacts in Table 13. We followed the intended use of all respective artifacts.

Table 13: **Licenses and sources for datasets and models used.** Datasets marked with * have no published license; the accompanying paper's arXiv license is used as fallback. Training entries marked with † or ‡ reflect compound or inferred licensing conditions.

Category	Name	License	Platform
Vision Encoder	SigLIP	Apache 2.0	Hugging Face
Language Model	LLaDA-8B	MIT	Hugging Face
Language Model	Dream-7B	Apache 2.0	Hugging Face
VLM	LLaVA-NeXT (1.6)	Apache 2.0	GitHub
VLM	LLaVA-NeXT (1.6)	LLaMA 2 License	Hugging Face
VLM	Open-LLaVA-NeXT	Apache 2.0	Hugging Face
Train Dataset	LLaVA-Pretrain	CC3M† + BSD-3-Clause	Hugging Face
Train Dataset	Open-LLaVA-NeXT-mix1M‡	CC BY-NC 4.0	Hugging Face
Evaluation Dataset	MME (MME-P)	arXiv Non-exclusive*	arXiv
Evaluation Dataset	VQAv2	CC BY 4.0	Official Website
Evaluation Dataset	MMBench	Apache 2.0	GitHub
Evaluation Dataset	MMMU	Apache 2.0	Hugging Face
Evaluation Dataset	MME (MME-C)	arXiv Non-exclusive*	arXiv
Evaluation Dataset	MathVista	CC BY-SA 4.0	Hugging Face
Evaluation Dataset	MathVerse	MIT	Hugging Face
Evaluation Dataset	MathVision	MIT	Hugging Face
Evaluation Dataset	ScienceQA	CC BY-NC-SA	Official Website
Evaluation Dataset	AI2D	arXiv Non-exclusive*	arXiv
Evaluation Dataset	TextVQA	CC BY 4.0	Official Website
Evaluation Dataset	DocVQA	arXiv Non-exclusive*	arXiv
Evaluation Dataset	ChartVQA	GPL-3.0	GitHub
Evaluation Dataset	InfoVQA	arXiv Non-exclusive*	arXiv

Note †: Subject to the CC-3M dataset may be freely used for any purpose, although acknowledgement of Google LLC ("Google") as the data source would be appreciated. The dataset is provided "AS IS" without any warranty, express or implied. Google disclaims all liability for any damages, direct or indirect, resulting from the use of the dataset

Note ‡: Our training data is based on Open-LLaVA-NeXT-mix1M, which combines ShareGPT4V data (CC BY-NC 4.0, research-only, with restrictions from LLaMA, Vicuna, and GPT-4 licenses) and AVG-LLaVA (Apache 2.0). All data was used strictly for academic research.

G LLM Usage

LLM is used to generate the math reasoning date for stage-3 training. See details in B.3.

H Concurrent Work

Concurrent to this work, MMaDa[78] (released after submission deadline) proposed a unified understanding and generation modeling using DM formulation. However, they do not leverage many of the novel techniques that we propose, leading to inferior performance and slow inference speed. We list a brief comparison in Table 14.

Table 14: **Comparison with MMaDa.** We report scores on MME, MMMU, and MMB benchmarks, along with average latency for image captioning.

Model	**MME**	**MMMU**	**MMB**	**Latency (s/image)**
LaViDa-Dream	**1463.5**	42.6	**73.8**	**1.13**
LaViDa-LLaDa	1365.6	**43.3**	70.5	1.32
MMaDa	1410.7	30.2	68.5	7.68